

# **Performance Analysis of Boost Converter using Soft Switching Schemes**

**A DISSERTATION**

**SUBMITTED IN PARTIAL FULFILLMENT OF THE  
REQUIREMENTS FOR THE AWARD OF THE DEGREE**

**OF**

**MASTER OF TECHNOLOGY**

**IN**

**POWER ELECTRONICS AND SYSTEMS**

**Submitted by:**

**ARIJIT NATH**

**2K24/PES/22**

**Under the supervision**

**PROF.DHEERAJ JOSHI**

**(Professor, EED, DTU)**



**DEPARTMENT OF ELECTRICAL ENGINEERING  
DELHI TECHNOLOGICAL UNIVERSITY**

**(Formerly Delhi College of Engineering)**

**Bawana Road, Delhi-110042**

**MAY 2026**

**M.Tech (Power Electronics and Systems)**

**ARIJIT NATH**

**2026**

**DEPARTMENT OF ELECTRICAL ENGINEERING**

**DELHI TECHNOLOGICAL UNIVERSITY**

(Formerly Delhi College of Engineering)

Bawana Road, Delhi-110042

## **CANDIDATE'S DECLARATION**

I, Arijit Nath, Roll No. 2K24/PES/22 student of MTech (Power Electronics & Systems), hereby declare that the project Dissertation titled “**Performance analysis of Boost Converter using Soft switching Schemes**” which is submitted by me to the Department of Electrical Engineering, Delhi Technological university, Delhi in partial fulfilment of the requirement for the award of the degree of Master of Technology, is original and not copied from any source without proper citation. This work has not previously formed the basis for the award of any Degree, Diploma Associateship, Fellowship, or other similar title or recognition.

**Place:** Delhi

**(Arijit Nath)**

**Date:** 30<sup>th</sup> May 2026

**DEPARTMENT OF ELECTRICAL ENGINEERING**  
**DELHI TECHNOLOGICAL UNIVERSITY**  
**(Formerly Delhi College of Engineering)**  
**Bawana Road, Delhi-110042**

**CERTIFICATE**

I hereby certify that the project Dissertation titled “**Performance analysis of Boost Converter using Soft Switching Schemes**” which is Submitted by Arijit Nath, Roll No. 2K24/PES/22, Department of Electrical Engineering, Delhi Technological University, Delhi in partial fulfilment of the requirement for the award of the degree of Master of Technology, is a record of the project work carried out by the student under my supervision. To the best of my knowledge, this work has not been submitted in part or full for any Degree or Diploma to this University or elsewhere.

**PROF.DHEERAJ JOSHI**

**Place:** Delhi

**Date:** 30<sup>th</sup> May 2026

**(SUPERVISOR)**

**DEPARTMENT OF ELECTRICAL ENGINEERING**

**DELHI TECHNOLOGICAL UNIVERSITY**

**(Formerly Delhi College of Engineering)**

**Bawana Road, Delhi-110042**

## **ACKNOWLEDGEMENT**

I would like to express my gratitude towards all the people who have contributed their precious time and effort to help me without whom it would not have been possible for me to understand and complete the project. I would like to thank **Prof. Dheeraj Joshi, DTU Delhi, Department of Electrical Engineering**, my Project Supervisor, for supporting, motivating, and encouraging me throughout this work carried out. His readiness for consultation always, his educative comments, and his concern and assistance even with practical things have been invaluable.

Finally, I must express my very profound gratitude to my parents, seniors, and my friends for providing me with unfailing support and continuous encouragement throughout the research work.

Date: 30<sup>th</sup> May,2026

**Arijit Nath**

**M.Tech (Power Electronics & Systems)**

**Roll No : 2K24/PES/22**

## ABSTRACT

The growing rate of renewable energy systems and electric vehicles' technology has driven the need for efficient DC-DC power converters. Boost converter is one of the attractive converter topologies that can step up the low input voltage to higher output voltage. The voltages generated by renewable energy sources, like PV systems and fuel cells, are typically low and variable in nature. Thus, effective techniques in voltage boosting is vital for the correct power conversion and utilization. Boost converters are commonly used in electric vehicle applications such as motor drive application and battery management system. The drawback of using conventional boost converter at high frequency is high switching losses. Such switching losses reduce efficiency and cause thermal stresses on semiconductor devices. To surmount these drawbacks, the soft switching techniques are adopted in the design of converter. Zero Voltage Switching (ZVS) and Zero Current Switching (ZCS) are two important soft-switching methods used in power electronics. These techniques minimize switching stress and enhance the efficiency of the converter. ZVS converters operate by switching element on and off when the voltage across the switch goes to zero. This minimizes switching losses and reduces electromagnetic interference. The switch is turned on when the current flows through the switch is zero, in ZCS converters. This lowers the stress and switching losses in operation. The present work is emphasizing on the design and analysis of different configuration of ZVS and ZCS boost converter. A variety of converter topologies are explored to study their performance characteristics. The proposed converters operate at high-frequency. The high frequency operation results in a reduction of the size of passive components (inductors and capacitors). But in the classical power converter high frequency switching results in high switching losses. Thus, soft switching techniques are necessary for an efficient operation. Various configurations of ZVS and ZCS boost converter in open loop condition are presented in the paper. The converters are modelled and simulated in MATLAB R2023a software. MATLAB Simulink is a flexible platform to analyse the behavior of the converter. The switching characteristics of these converters are better understood by simulating them. Different parameters like output voltage, current waveform, switching stress and efficiency are studied. The voltage stress of switching devices are reduced in

the proposed ZVS converter configuration. Likewise, the ZCS converter configuration shows a lower current stress during switching transitions. Switching waveforms are used to check the implementation of the soft switching conditions. The switching loss is reduced, which leads to an improvement of the overall efficiency of the converter system. The converters also have smoother voltage and current waveforms than the conventional converters. Switching stress is reduced and the reliability and lifespan of semiconductor devices are improved. For renewable energy applications where efficiency is a key concern, soft switching converters are very appropriate. Boost converters are employed for the connection between the solar panels and the DC buses in the PV systems or with the battery systems. Such applications can be enhanced in terms of power conversion efficiency by the proposed converters. For a battery powered system, an efficient DC-DC conversion is essential in an electric vehicle. The soft-switching boost converters designed can help in energy saving in EV systems. The simulation results match the stable operation of the converter topologies under the various operating conditions. Successful regulation of the output voltage is obtained in open loop mode. The resonant components used in the converter help in achieving soft-switching conditions. Efficient operation of the converter requires the proper design of its resonant inductors and capacitors. Operating principle of various converter configurations are also discussed. Switching sequences are analyzed in detail to get insight to the converter performance. The voltage and current waveforms simulated agree with the theoretical analysis. The proposed converter configurations can offer higher efficiency than hard switched converter. Lower switching losses results in decreased heat generation in the converter circuit. This makes the need for big heat sinks and cooling systems unnecessary. Consequently, the entire converter system is compact and economical. The study shows that soft-switching techniques are greatly beneficial in the modern power electronic system. The designed converter models can be further expanded on for the closed loop control analysis. Advanced controllers for voltage regulation and stability improvement can be implemented in the future. The proposed work helps in the development of efficient DC-DC conversion for renewable energy and EVs applications. The study emphasizes that in order to reduce switching losses and increase the efficiency, ZVS and ZCS techniques are important. Thus, soft-switching boost converter is a potential solution to future sustainable energy

## Table of Contents

CANDIDATE'S DECLARATION .....	ii
CERTIFICATE .....	iii
ACKNOWLEDGEMENT .....	iv
ABSTRACT .....	v
LIST OF FIGURES .....	x
LIST OF TABLES.....	xii
LIST OF ABBREVIATIONS.....	xiii
CHAPTER 1.....	1
1.1 Overview.....	1
1.2 Introduction to Soft Switching based Boost Converter.....	2
1.3 Thesis Motivation. ....	3
1.4 Literature Review .....	4
CHAPTER 2.....	8
DESIGN OF ZVS BOOST CONVERTER.....	8
2.1 Introduction .....	8
2.2 Working of ZVS Boost Converter.....	9
2.2.1 Mode I Operation ( $0 < t < t_1$ ).....	9
2.2.2 Mode II Operation ( $t_1 < t < t_2$ ).....	10
2.2.3 Mode III Operation ( $t_2 < t < t_3$ ) .....	11
2.2.4 Mode IV Operation ( $t_3 < t < t_4$ ) .....	12
CHAPTER 3 .....	14
MODELING OF ZVS BOOST CONVERTER.....	14
3.1 Introduction .....	14
3.2 DC Voltage Transfer Function .....	15
CHAPTER 4.....	16
DESIGN OF COMPONENT OF ZVS BOOST CONVERTER .....	16
4.1 Introduction .....	16
4.2 Equation for Resonating Inductor ( $L_{cr}$ ).....	17
4.3 Equation for Resonating Capacitor ( $C_{cr}$ ) .....	17
4.4 Equation for Filter Capacitor ( $C_c$ ) .....	17
4.5 Equation for Filter Inductor ( $L_c$ ).....	17

<b>CHAPTER 5</b> .....	<b>19</b>
<b>Design PI Controller for ZVS Boost Converter</b> .....	<b>19</b>
<b>5.1 Introduction</b> .....	19
<b>5.2 Design of PI Controller for Boost Converter</b> .....	21
<b>5.3 Proportional Action (<math>K_P</math>)</b> .....	22
<b>5.4 Integrating Action (<math>K_i</math>)</b> .....	23
<b>5.5 Combine effect of PI Controller</b> .....	24
<b>5.6 Deriving State Space Averaging Equation</b> .....	25
<b>5.7 Deriving Small Signal Model for Boost Converter</b> .....	27
<b>5.3 Finding <math>K_p</math> and <math>K_i</math> value for PI Controller</b> .....	27
<b>CHAPTER 6</b> .....	<b>29</b>
<b>TYPES OF ZVS BOOST CONVERTER</b> .....	<b>29</b>
<b>6.1 M-type Half-wave ZVS Boost Converter</b> .....	29
<b>6.2 M-type Full-wave ZVS Boost Converter</b> .....	30
<b>6.4 L-type Full-wave ZVS Boost Converter</b> .....	31
<b>CHAPTER 7</b> .....	<b>32</b>
<b>DESCRIPTION OF THE ZCS BOOST CONVERTER &amp; OPERATING PRINCIPAL</b> .....	<b>32</b>
<b>7.1 Overview</b> .....	32
<b>7.2 Half-wave ZCS Boost Converter operating principal</b> .....	32
<b>7.3 Full-wave ZCS Boost Converter operating principal</b> .....	33
<b>CHAPTER 8</b> .....	<b>34</b>
<b>RESULT &amp; DISCUSSION</b> .....	<b>34</b>
<b>8.1 ZVS-Boost Converter performance in open loop</b> .....	34
<b>8.2 Load Regulation of ZVS Boost Converter in open loop</b> .....	35
<b>8.3 ZVS Boost Converter performance using PI controller</b> .....	36
<b>8.4 Load Regulation of ZVS Boost Converter using PI Controller</b> .....	37
<b>8.5 Compared results of different ZVS Switching schemes</b> .....	38
<b>8.6 Switching Current comparison between ZVS &amp; ZCS Boost Converter</b> .....	40
<b>8.7 Switching Voltage comparison between ZVS &amp; ZCS Boost Converter</b> .....	40
<b>8.8 SIMULATION BASED RESULT</b> .....	41
<b>8.9 Discussion</b> .....	43

**CHAPTER 9 .....44**  
    **9.1 Conclusion ..... 44**  
    **9.2 Future scope ..... 46**  
**REFERENCES.....47**  
    **List of Publications ..... 49**

## LIST OF FIGURES

<b>Figure No.</b>	<b>Figure Name</b>	<b>Page No.</b>
Figure No.1	Schematic diagram of ZVS Boost Converter	2
Figure No.2	Short circuited capacitor and input voltage source and open circuit for inductor	3
Figure No.3	Switch and diode are on	8
Figure No.4	Switch is on and Diode off	9
Figure No.5	Both switch and diode are off	10
Figure No.6	Switch is off and Diode is on	11
Figure No.7	Schematic diagram of a Boost Converter	12
Figure No.8	Simulation of ZVS Boost converter using PI	15
Figure No.9	Schematic diagram for M-type Halfwave ZVS Boost Converter	17
Figure No.10	Steady state wave from M-type Half-wave Boost Converter	18
Figure No.11	Circuit diagram of M-type Full-wave ZVS Boost Converter	19
Figure No.12	Steady state waveform of M-type Full-wave Boost converter	20
Figure No.13	Circuit diagram of L-type Half-wave ZVS Boost converter	20
Figure No.14	Steady state waveform L-type Half-wave ZVS Boost converter	21
Figure No.15	Circuit diagram of L-type Full-wave ZVS Boost Converter	20

Figure No. 16	Steady state waveform L-type Full-wave ZVS Boost converter	20
Figure No.17	Circuit diagram of Half-wave ZCS Boost converter	21
Figure No. 18	Steady state waveform of Half-wave ZCS Boost converter	21
Figure No.19	Circuit diagram of Full-wave ZCS Boost Converter	22
Figure No.20	Steady-state wavefrom of Full-wave Boost Converter	22

## LIST OF TABLES

<b>Table No.</b>	<b>Table Name</b>	<b>Page No.</b>
Table 1	Design of Components parameters of ZVS Boost Converter	15
Table 2	Parameters are considered for Converters	32

## LIST OF ABBREVIATIONS

QRC	Quasi Resonant Converter
PI	Proportional Intrigal
PV	Photovoltaic
EV	Electric Vehicle
PWM	Pulse Width Modulation
EMI	Electromagnetic Interference
ESR	Equivalent Series Resistances
ZVS	Zero Voltage Switching
ZCS	Zero Current Switching
SiC	Silicon Carbide
GaN	Gallium Nitride

# CHAPTER 1

## INTRODUCTION

### 1.1 Overview

The Zero Voltage Switching (ZVS) boost converter is a soft switching DC-DC converter, which is very popular in high-frequency power conversion applications for reducing switching losses and enhancing the power conversion efficiency. The switching stress is reduced, the power dissipated in the semiconductor switch is reduced and the overall efficiency is improved in a ZVS converter by turning the semiconductor switch ON when the voltage across the switch is almost zero. The conventional hard-switched boost converter suffers from high switching losses and EMI at high switching frequencies; ZVS boost converter by using resonant or auxiliary circuits, can eliminate these shortcomings, realize soft-switching. The choice of ZVS boost converter is primarily based on efficiency, frequency, power rating, and the mode of application. The high efficiency and compact design make these converters a popular choice in various renewable energy applications, electric vehicle chargers, telecom power supplies, industrial power systems, and modern data centers. One of the most crucial parameters when selecting a ZVS boost converter is its switching frequency. The higher the switching frequency, the smaller the passive components, like inductors and capacitors, and thus the smaller the converter design. But, high frequency operation comes with switching losses in the conventional converters and therefore ZVS techniques are very helpful. Selection of semiconductors is also very important. MOSFETs are preferred by virtue of their fast switching speed, while SiC and GaN devices are more popular in high frequency and efficiency applications because of their excellent switching performance. To ensure stable operation, the designer should take into account the input voltage range, the required output voltage, the load conditions and the duty cycle run.

## 1.2 Introduction to Soft Switching based Boost Converter

Conventional pwm converter switches the voltage and currents of semiconductor devices from high level to 0 or 0 to high level quickly in turn on or turn off, that cause the switching losses, and produce a large amount of electromagnetic wave radiation interference[1]. Currently, it is not possible to achieve the ideal performance of the PWM converter architecture using semiconductor power devices and magnetic components. Switching losses are due to the output capacitance of the transformer, the capacitance of the diodes, the reverse recovery of the diodes, and the leakage inductance of the transformer [2].The energy storage in transistor as output capacitance before the transistor on When transistor turns on, this energy is lost in the transistor, resulting in the transistor switching losses.[3] As switching losses are directly related to switching frequency, they limit maximum switching frequency. The wide range of harmonics seen in the rectangular PWM waveform is the cause of the high amount of EMI [4]. High current spikes due to diode reverse recovery cause a variety of harmonics, and leakage of transformer inductance from resonant circuits with the transistors and diode output capacitance causes Ringing in isolated converters [5].Although the soft switching methods can reduce EMI and switching losses for dc-dc power converters, it brings up the conduction losses and strains of devices. Switching losses are avoided because the product of the device voltage and current during the switching process is zero, as the semiconductor devices are turned on or off at zero voltage and/or zero current [6]. With less reactive components, the soft switching converter can be lighter and have a higher switching frequency There is less EMI because the current and voltage wave's harmonic content is decreased [7]. The soft switching methods can be classified into two types as (a) Zero voltage switching (ZVS) and (b) Zero current switching (ZCS)[8]. In ZVS, the voltage across the transistor will be zero when it is switched on. Therefore, no switching losses due to the output capacitance, which stores no energy in the transistor, occur when the switching is done.This means that no switch-on losses occur since the output capacitance, which stores no energy in the switch, is not switched on when switching takes place.Soft switching converter absorbs

many parasitics components like transistors output capacitance, diode capacitance and transformer leakage inductance[10].Zero voltage transistor turn on (ZVS) is a technique used in the ZVS.

### **1.3 Thesis Motivation.**

This research work is motivated by the growing requirement of efficient DC-DC power converter in renewable energy systems, EVs and the modern power electronic applications. The main problem of conventional boost converter is that under high frequency operation, switching losses are high. Such switching losses decrease the overall efficiency of the converter. The high switching frequency also causes electromagnetic interference and thermal stress of semiconductor devices. Hence, soft switching techniques are a major area of research interest because of these issues. One of the most significant soft switching method is the Zero Voltage Switching (ZVS). In ZVS converter, the switch is turned on at zero voltage. This will greatly cut down on switching loss. It also also decreases stress to the MOSFET switch. Reduced switching stress increases converter reliability and increases converter life. The other significant benefit of ZVS operation is that it helps in minimizing the emission of EMI. The harmonics are reduced, which leads to a better performance of the converter. Thus, ZVS boost converters are appealing for applications at high frequencies. But avoiding fluctuations in the output voltage when the load changes remains a challenge. Open-loop converters do not provide an adequate control over voltage under varying operating conditions. Due to this constraint, closed-loop control techniques are needed. In comparison to other controllers, the PI controller is widely used due to its simplicity in structure and good dynamic response. The PI controller is able to minimize the steady state error and enhance the voltage regulation. In this research paper, the proposal and analysis of a PI controlled ZVS boost converter is presented. The converter has an input of 21.6V and an output of 48V. Switching frequency is decided to be 50 KHz. Care is taken in designing resonant components like resonant inductor and resonant capacitor to obtain the ZVS operation. Various operating modes are used to explain the converter operation. Also, a mathematical analysis of each mode is provided. ZVS boost converter is modeled to enhance the understanding of the converter behavior. A transfer function of the boost converter is

obtained for controlling the converter. Parameters of the PI controller are designed to achieve better transient response and voltage stability. The proposed system is simulated and validated using MATLAB/Simulink. The simulation results confirm that the converter is able to deliver a stable output voltage. The proposed converter also exhibits minimal switching stress on the MOSFET. In open loop configuration, the output voltage varies considerably as a function of load. The voltage regulation has improved significantly after applying the PI controller. The output voltage is stable around 48V. The output current is also more stable in situations where there is a load disturbance. The proposed controller is able to cope with load variation conditions. The voltage ripple is reduced after applying the controller. One more significant note is that the voltage of the switch decreases during closed-loop mode. This means the switching losses have decreased. Switching losses are lowered, which increases converter efficiency. Reduced switch voltage also reduces heating of the device. This can lead to a decrease in MOSFET switch failure rate. The proposed work can thus enhance the reliability of the converter system. The performance of the proposed ZVS boost converter is better than conventional converter. The study also emphasizes the role of the control methods in the soft switching of a converter. The proposed methodology can be used in renewable energy applications. It can also be used in the EV power conversion systems. The work proves that ZVS boost converter is easily controlled by PI control. This study includes detailed design procedures of resonant components and controller parameters. The converter performance is tested under various operating conditions. Results are validating stability and robustness of the system. The proposed converter is better loaded regulated as compared to open-loop systems. This research is therefore helpful in designing efficient and reliable power electronic converter.

#### **1.4 Literature Review**

Work on soft-switching DC-DC converter commenced with the invention of zero-voltage switching (ZVS) techniques for the conversion of a DC input voltage to another DC voltage by K. Liu and F. C.

Lee in 1986. they investigated a way in which by turning on the switches at zero-voltage switching intervals the loss, switching stress in the DC-DC converters switching at high

frequencies could be reduced. This innovation paved the way for various topologies of the modern soft-switching converter designs that allow for converter operation at higher frequencies. In the similar time period, M.

K. Kazimierczuk and J. Jzwik proposed new topologies of high-efficiency high-frequency ZVS resonant DC-DC converters in which their research on resonant networks for soft switching and for minimal switching loss power dissipation.

The authors showed various novel concepts in which these type of high-efficiency resonant power converters can achieve higher frequencies, reduce EMI, and decrease switching loss. The design of the new soft-switching dc-dc topologies can be viewed with the aid of analysis performed with the use of practical issues addressed via the theory and the commercial software program for layout and implementation by way of P. C.

Todd and R. W. Lutz.

In addition, Kazimierczuk and Jzwik provided the analysis and design of a buck ZVS resonant converter that became a guideline inside the improvement of those topologies. Kazimierczuk and W. D.

Morse did analysis of the use of state-plane analysis of ZVS resonant converter in 1989. Their article presents the concept of the use of the state plane to review the dynamics of dc-dc converters. Kazimierczuk continued research of ZVS boost converter by stating its capabilities via a design-directed approach to analyze the.

ZVS-ZCS topologies later on, were investigated and used for the converter topologies. Soft-switching converter design for the renewable energy applications by using B. R.

Lin and Fang-Yu Hsieh, with their active clamp circuit ZVT converter for zero-voltage turn on. Control issues, voltage mode PID control for Cuk converters were examined by P. S.

Shandilya et al., which was able to improve the operation of closed-loop converter. A PI-controlled soft switching boost converter design and experiment with its results was reported by P. Usha & Priyanka K in 2015.

Dheeraj Joshi et al designed high-efficiency boost dc-dc converter for photovoltaic solar systems that provide a solution in voltage up-conversion and minimized power loss. Dr Robert W. Erickson and Prof Dr.agan Maksimovic published an important textbook that provides a clear concept of power electronic converters theory, Small-signal modeling and control, and resonant converters which could provide fundamental basis of the topic of converter design and controller structure.

Zero voltage transition (ZVT) DC-DC boost converter with efficient EMI reduction and higher efficiency by Genesis C. Tavares and Noah Dias was a notable modern contribution. Research on adaptive ZVS boost converter by Souhali Barakat et al. was an attempt to design more stable converter for varying conditions.

Design and control of a PI controller based ZVS boost converter was reported by Arijit Nath and Dheeraj Joshi with MATLAB/Simulink simulation results and it also shows that with this converter efficiency gets improved and losses reduced. M. J.

Baig and R. K. Singh presented a design and analyzed ZVS-ZCS boost converter with improved performance characteristics (reduced switching losses, EMI, switching stresses)

Although the ZVS and ZCS boost converter topologies have been highly developed, there are still some key research challenges associated with soft switching boost DC-DC converter topologies. The majority of the previous works focused on soft switching and converter efficiency, with comparatively less emphasis being placed on the closed-loop control performance, dynamic stability, and practical issues. The real-time performance of the converter is limited by the parasitic elements, the component tolerances, thermal effects and electromagnetic interference, and many existing studies are based on ideal operating conditions without considering such factors. While voltage regulation using PI and PID controllers are commonly employed for the ZVS boost converter, the modelling of the small signal, stability analysis and transient response under various load and input conditions is still limited. For a variety of proposed soft switching converters, the extra resonant and auxiliary circuits result in higher component counts, design complexity and cost, making them impractical for small and inexpensive applications. In addition, there has been little research on simultaneous optimization of efficiency, EMI reduction,

switching stress and dynamic response. Experimental hardware validation and real time implementation are relatively few, while most research contributions are validated by MATLAB simulation. The advanced control methods like fuzzy logic control, sliding mode control, adaptive control, artificial intelligence based control, and model predictive control have not been studied extensively in ZVS and ZCS boost converter. Furthermore, there is only a few limited studies on converter performance as function of light load, parameter variations and operation at high frequencies. The integration of soft-switching boost converters in renewable energy systems, in PV systems, in electric vehicle charging systems and in smart-grid infrastructures is also under development. Hence, it is highly required to conduct further research on the simpler, high power conversion efficiency, closed-loop controlled ZVS/ZCS boost converter with better stability, lower EMI, switching losses, and better transient response and of the actual hardware implementation for modern sustainable energy

## CHAPTER 2

### DESIGN OF ZVS BOOST CONVERTER

#### 2.1 Introduction

These converter are obtained by adding a resonant capacitor  $C_r$  in parallel with the switch and resonant inductor  $L_r$  in series with the parallel combination of switch and resonant capacitor[2]. The transistor or switch output capacitance is absorbed into the  $C_r$ . The diode lead inductance is absorbed into the  $L_r$ . An anti-parallel diode found in power MOSFETs prevents a switch voltage of less than  $-0.7V$  [2]. This type of switch is bidirectional for current and unidirectional for voltage. Half-wave ZVS converters are ZVS quasi-resonant converters with a unidirectional voltage switch. To prevent a  $-Ve$  switch voltage, a diode might be connected in series with the transistor[3]. This type of switch is unidirectional for current and bidirectional for voltage. The full-wave ZVS converter is a ZVS quasi resonant converter that has a unidirectional switch for current and a bidirectional switch for voltage. Figure 2; displays a high frequency for the equivalent circuit of a ZVS converter. Low-frequency and dc components are reduced to zero to obtain the circuit. The input dc source  $V_{in}$  is substituted with a short circuit, the filter capacitance  $C$  is substituted with a short circuit, and the filter inductor  $L$  is substituted with an open circuit[8].

In the Fig (1.a) looks like  $L_r$ - $C_r$  circuit,

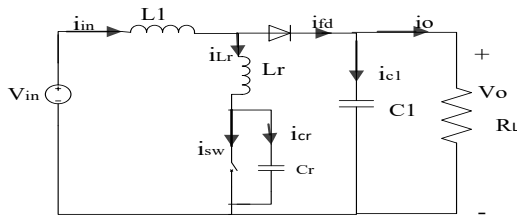


Fig2.1 : Schametic diagram of ZVS Boost Converter voltage

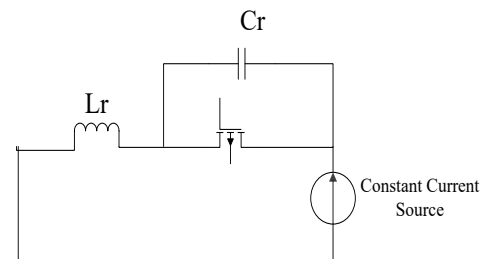


Fig 2.2: Short circuited capacitor and input source and open circuit for inductor[2]

$$\text{resonant frequency } \omega_0 = \frac{1}{\sqrt{L_r C_r}} \quad (2.1)$$

$$\text{Normal switching frequency } A = \frac{f_s}{f_0} \quad (2.2)$$

The load quality

$$Q = \frac{R_L}{\omega_0 L_r} = \omega_0 C_r R_L = \frac{R_L}{\sqrt{\frac{L_r}{C_r}}} = \frac{A R_L}{\omega_s L_r} \quad (2.3)$$

## 2.2 Working of ZVS Boost Converter

Initially, both the switch and diode conduct. The voltage across the switch is zero. The resonant inductor current starts increasing linearly, energy is stored in the resonant inductor. When the diode becomes reverse biased and turns OFF. The input source transfers energy through the resonant inductor and switch. The resonant capacitor voltage begins changing because of resonance between  $L_r$  and  $C_r$  [6]. When the switch is turned OFF. The resonant capacitor charges and the switch voltage rises gradually instead of suddenly. Because of resonance, the voltage and current waveforms become sinusoidal. The capacitor and inductor exchange energy during this interval. The switch voltage eventually reaches its peak value. When the diode turns ON and transfers stored energy to the load. The resonant capacitor discharges. Due to resonance, the switch voltage decreases toward zero. When the switch voltage becomes zero, the MOSFET is turned ON again. This achieves Zero Voltage Switching [11].

### 2.2.1 Mode I Operation ( $0 < t < t_1$ )

For the resonant inductor charging in the interval  $0 < t < t_1$ ; both switch and diode are on. See in Fig3

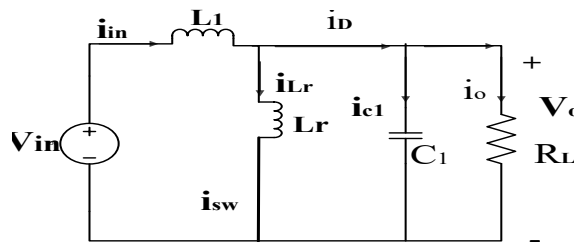


Fig 2.3: Switch and diode are on

During this time interval,  $V_{sw}=0$ ,  $v_D=0$ ,  $i_C=0$ ,  $V_{Lcr}=V_o$ . And

$$\begin{aligned}
 i_{Lcr} &= \frac{1}{w_s L_{cr}} \int_0^{w_s t} v_{Lcr} d(w_s t) + i_{Lcr}(0) \\
 &= \frac{V_0}{w_s L_{cr}} w_s t + i_s(0)
 \end{aligned} \tag{2.4}$$

Since  $V_0 = I_0 R_L$  and

$$\frac{V_0}{w_s} \times \frac{1}{L_{cr}} = \frac{I_{in} Q}{M_{VDC} A} \tag{2.5}$$

$$\frac{i_{Lcr}}{I_{in}}(w_s t) = \frac{i_{sw}(w_s t)}{I_{in}} = \frac{Q \cdot w_s t}{AM_{VDC}} + h \tag{2.6}$$

The diode current is given by

$$\frac{i_D(w_s t)}{I_{in}} = -\frac{Q}{AM_{VDC}} w_s t - h + 1 \tag{2.7}$$

At the end of this time interval,  $i_D(w_s t_1) = 0$ ;

Hence ,

$$w_s t_1 = \frac{AM_{VDC}}{Q} (1 - h). \tag{2.8}$$

### 2.2.2 Mode II Operation ( $t_1 < t < t_2$ )

For time interval  $t_1 < t \leq t_2$  , the switch is on and diode is off. The converter model is shown in bellow Fig 4; During this time interval  $V_{sw} = 0, i_{cr} = 0, i_D = 0, v_{Lcr} = 0, i_{Lcr} = i_{sw} = I_{in}$ , and  $v_D = -V_0$ .

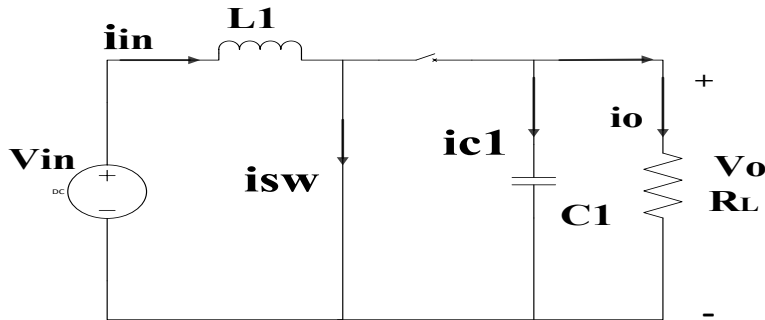


Fig2.4: Switch is on and Diode off

### 2.2.3 Mode III Operation ( $t_2 < t < t_3$ )

During time interval  $t_2 < t \leq t_3$ , both switch and diode are off. This time interval  $i_{sw} = 0, i_D = 0, i_{Lcr} = i_{cr} = I_{in}, v_{Lcr} = 0$ .

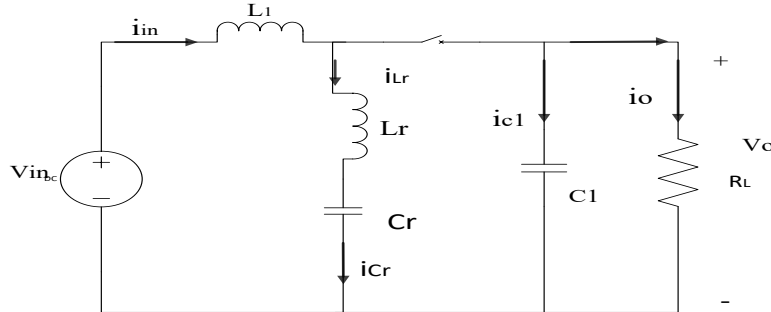


Fig2.5: Both switch and diode are off

$$V_{sw} = \int_{t_2}^{w_s t} v_{cr} d(w_s t) + v_{cr} t_2; \quad (2.9)$$

Let assume  $t_2 = 2\pi D$ ;

$$\begin{aligned} V_{sw} &= \int_{2\pi D}^{w_s t} v_{cr} d(w_s t) + v_{cr}(2\pi D); \\ &= \frac{I_{in}}{w_s C_r} (w_s t - 2\pi D). \end{aligned} \quad (2.10)$$

Because  $\frac{I_{in}}{w_r C_r} = \frac{M_{VDC} V_0}{AQ}$ ; and  $I_0 = \frac{V_0}{R_L}$

We get

$$\frac{v_{sw}}{V_0} = \frac{M_{VDC}}{AQ} (w_r t - 2\pi D); \quad (2.11)$$

$$v_D / V_0 = \frac{M_{VDC}}{AQ} (w_r t - 2\pi D) - 1; \quad (2.12)$$

The end of this time interval is determined by putting  $v_D(wt_3) = 0$ .

$$w_s t_3 = 2\pi D + \frac{AQ}{M_{VDC}}. \quad (2.13)$$

### 2.2.4 Mode IV Operation ( $t_3 < t < t_4$ )

Now  $t_3 < t \leq T$ ; the switch is off and diode is on. This time interval  $i_{sw} = 0$  and  $v_D = 0$ . Initial condition are  $i_L(w_s t) = I_{in}$  and  $v_{sw}(w_s t_3) = V_{in}$ .

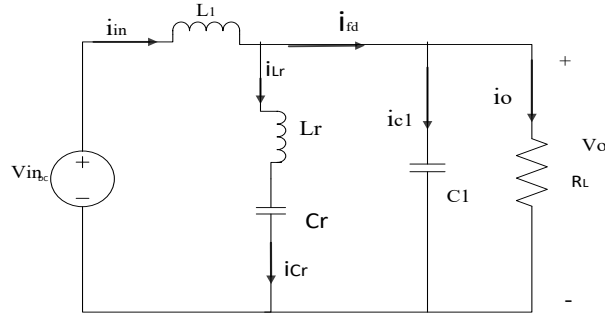


Fig2.6: Switch is off and Diode is on

Using Laplace Transform,

$$i_{Lr}(s) = \frac{s}{s^2 + \omega_0^2} I_{in} e^{-st_3}. \quad (2.14)$$

$$\frac{i_{Lr}}{I_{in}} = \frac{i_{Cr}}{I_{in}} = \cos \frac{\omega_s t - \omega_s t_3}{A} \quad (2.15)$$

Diode current is,

$$\frac{i_D}{I_{in}} = 1 - \cos \frac{\omega_s t - \omega_s t_3}{A}; \quad (2.16)$$

Since  $I_o = \frac{V_o}{R_L}$  and  $\frac{\omega_s L_r I_{in}}{A} = \frac{V_o M_{VDC}}{Q}$ ;

We have,

$$v_L = \omega_s L \frac{di_L}{d(\omega_s t)} = \frac{M_{VDC}}{Q} \sin \frac{\omega_s t - \omega_s t_3}{A};$$

Switch voltage,

$$\frac{V_{sw}}{V_{in}} = \frac{M_{VDC}}{Q} \sin \frac{\omega_s t - \omega_s t_3}{A} + 1; \quad (2.17)$$

For *zvs* operation  $V_{SW}(2\pi) = V_{SW}(0) = 0$ ; and  $i_{Lr}(2\pi) = i_{Lr}(0) = I_0$ .

Hence the relation among  $M_{VDC}$ ,  $Q$  and  $h$  are given by,

$$h = \cos\left[\frac{2\pi(1-D)}{A} - \frac{Q}{M_{VDC}}\right], \quad (2.18)$$

$$\text{and } \frac{Q}{M_{VDC}} = -\sin\left[\frac{2\pi(1-D)}{A} - \frac{Q}{M_{VDC}}\right], \quad (2.19)$$

$$h = \sqrt{1 - \left(\frac{Q}{M_{VDC}}\right)^2}, \quad (2.20)$$

The duty cycle,

$$D = 1 - \frac{1}{2\pi} \left(\frac{f_s}{f_0}\right) [2\pi n - \arccos h + \sqrt{1 - h^2}], \quad (2.21)$$

For  $n=1$  and  $h=0$ ,

$$D = 1 - \frac{3\pi+2}{4\pi} \left(\frac{f_s}{f_0}\right); \quad (2.22)$$

$$D = 1 - 0.9092 \left(\frac{f_s}{f_0}\right); \quad (2.23)$$

## CHAPTER 3

### MODELING OF ZVS BOOST CONVERTER

#### 3.1 Introduction

Modeling of a ZVS boost converter is very crucial as it helps in understanding, analysis, design and control of the converter well. The resonant components, along with switching devices and (nonlinear characteristics) make it difficult to foresee the behavior of the converter without modeling without a ZVS boost converter. Mathematical representation of a converter by modelling using equations and transfer functions is helpful in analysing the voltage, current, duty cycle and switching performance. The main application is in the design of controllers such as PI or PID controller because the transfer function of the converter plays an important role in the design of such controllers. Modeling can be used by engineers to explore the stability of the converter and to see if the system will function correctly for various inputs and loads. It also allows for the analysis of the transient response and its characteristics such as rise time, settling time, overshoot and steady state error during rapid load and/or source voltage changes. Resonant inductors and capacitors also are playing important role in ZVS boost converter so modeling of the same is required for selecting the appropriate values of the resonant components for ZVS (zero voltage switching) condition. The voltage and current waveforms across the switch are also provided, which makes it easier to analyse the losses and the reduction in the converter efficiency, and makes it possible to minimise these losses by using modelling. This is useful as a check to make sure that the MOSFET can be turned on at zero voltage, which is the main objective of ZVS operation. Another need of modeling is simulation in software prior to the implementation such as MATLAB/Simulink. Using simulation based on modelling can reduce the cost of using hardware, reduce risk in experiments and reduce the development time. Using the modeling, the study of the load regulation performance and line regulation performance of the converter can also be obtained. Other helpful frequency analysis information such as bode plot, crossover frequency, gain margin and phase margin can be modeled as well. Furthermore, the modeling can be used to predict voltage ripple, current ripple, switch stress and overall dynamic response of the converter. Therefore, the modeling of ZVS boost converter is required in the following applications:

designing the ZVS boost converter, stability analysis of the converter, efficiency improving of the converter, converter performance prediction, and implementing of the ZVS boost converter in renewable energy system, EV application and high frequency power electronic system.

### 3.2 DC Voltage Transfer Function

Modeling a ZVS boost converter is crucial for understanding, designing, and optimizing both the circuit and its closed-loop control, directly supporting higher voltage regulation, stability, and practical deployment.

$$I_o = I_{in} \left[ 1 - D + \frac{1-h^2}{4\pi\sqrt{1-h^2}} \right] \quad (3.1)$$

Assuming that the converter is lossless,  $I_o V_o = I_{in} V_{in}$ .

Hence, the dc voltage transfer function is given by

$$M_{VDC} = \frac{V_o}{V_{in}} = \frac{I_{in}}{I_o} = \frac{1}{1-D + \frac{A(1-h^2)}{4\pi\sqrt{1-h^2}}} = \frac{2\pi}{A[2\pi n - \arccos h + \sqrt{1-h^2} + \frac{(1-h^2)}{2\sqrt{1-h^2}}]} \quad (3.2)$$

Thus, for  $h \leq 0$ ;

$$M_{VDC} = \frac{2\pi}{\left(\frac{f_s}{f_0}\right) \left\{ (2n-1)\pi + \frac{Q}{M_{VDC}} + \arccos \sqrt{1 - \left(\frac{Q}{M_{VDC}}\right)^2} + \frac{M_{VDC}}{2Q} \left[ 1 + \sqrt{1 - \left(\frac{Q}{M_{VDC}}\right)^2} \right] \right\}} \quad (3.3)$$

And for  $h \geq 0$ ;

$$M_{VDC} = \frac{2\pi}{\frac{f_s}{f_0} \left\{ 2n\pi + \frac{Q}{M_{VDC}} - \arccos \sqrt{1 - \left(\frac{Q}{M_{VDC}}\right)^2} + \frac{M_{VDC}}{2Q} \left[ 1 - \sqrt{1 - \left(\frac{Q}{M_{VDC}}\right)^2} \right] \right\}} \quad (3.4)$$

Now Putting  $n=1$  and  $h=0$ ;

$$M_{VDC} = \frac{1}{1-D} = \frac{4\pi}{(3\pi+2)\left(\frac{f_s}{f_0}\right)} = \frac{1.1}{\left(\frac{f_s}{f_0}\right)}; \quad (3.5)$$

## **CHAPTER 4**

### **DESIGN OF COMPONENT OF ZVS BOOST CONVERTER**

#### **4.1 Introduction**

When designing a ZVS boost converter, the design of its components is highly critical, since the performance of the converter relies on the proper choice of components. Careful design of components like resonant inductor, resonant capacitor, filter inductor, filter capacitor, MOSFET and diode is necessary in a ZVS boost converter. Zero voltage switching operation can be achieved through proper design of the components. In ZVS operation, the MOSFET will switch on with a zero voltage, thus minimizing the switching losses. Wise design of resonant components contributes to achieve resonance between the voltage and current wave forms. This resonance helps to minimize the stress on the MOSFET during switching. Appropriate component selection also leads to a better converter efficiency. The resonant frequency is a function of the values of the resonant inductor and resonant capacitor. The filter inductor and capacitor are used to lower the output voltage and current ripple. Appropriate components value is used to ensure a stable output voltage under different load conditions. Proper design can also minimize electromagnetic interference within the converter. The voltage and current stress are considered in the selection of the MOSFET and the diode ratings. The values of the components may be incorrect, resulting in instability and heating. The proper design can enhance the converter's transient response. It also decreases conduction losses and switching losses. The design of the components plays an important role in achieving its desired output voltage and power rate. Good design of components enhances reliability and the life of the converter. Before simulation and hardware implementation, it is also important to correct the design of the components. Therefore, the design of the components is crucial to the efficient, stable and reliable operation of a ZVS boost converter.

## 4.2 Equation for Resonating Inductor ( $L_{cr}$ )

For design of components of ZVS Boost converter, input voltage is taken as 21.6V, output voltage as 48V and switching frequency( $f_{sw}$ ) as 50 kHz respectively.

$$R_L = \frac{V_0}{I_0} = 7.05\Omega \quad M_{VDC} = Q = \frac{V_0}{V_{in}} = 2.22$$

$$L_{cr} = \frac{R_L}{\omega_0 Q} = 5.01 \times 10^{-6} H$$

## 4.3 Equation for Resonating Capacitor ( $C_{cr}$ )

$$C_{cr} = \frac{Q}{\omega_0 R_L} = 5 \times 10^{-7} F$$

## 4.4 Equation for Filter Capacitor ( $C_c$ )

$$D = 1 - 0.9092 \left( \frac{f_{sw}}{f_0} \right) = 0.549 = 54.9\% = 55$$

$$C_{c_{min}} = \frac{D}{2f_s R} = 7.80 \times 10^{-7} F$$

But Filter Capacitor can be taken as  $C_c > C_{c_{min}}$ ;  $C_c = 8 \times 10^{-6} F$ .

## 4.5 Equation for Filter inductor ( $L_c$ )

$$L_{c_{min}} = \frac{R(1-D)^2 D}{2f_s} = 7.85 \times 10^{-6} H$$

Similarly, for filter inductance  $L_c > L_{c_{min}}$ ;  $L_c = 180 \times 10^{-6} H$

Input Voltage $V_{in}$ (V)	<b>21.6</b>
Output Voltage $V_0$ (V)	48
Switching frequency $f_{sw}$ (kHz)	50
Resonant frequency $f_0$ (kHz)	101
Duty ratio (D)	55
Load Quality (Q)	2.22
DC Voltage transfer function ( $M_{VDC}$ )	2.22
Load Resistance $R_L$ ( $\Omega$ )	7.05
Resonating Capacitor $C_{cr}$ (F)	$5 \times 10^{-7}$
Resonating Inductor $L_{cr}$ (H)	$5 \times 10^{-6}$
Filter Inductor $L_c$ (H)	$180 \times 10^{-6}$
Filter Capacitor $C_c$ (F)	$8 \times 10^{-6}$

Table1: Design of Components parameters of ZVS Boost Converter

## CHAPTER 5

### Design PI Controller for ZVS Boost Converter

#### 5.1 Introduction

Control of a boost converter is important for the performance and stability of the converter. Because the boost converter is a high-frequency switching converter, its dynamics will be nonlinear, it is important to have a proper controller to ensure a regulated and stable output voltage for different operating conditions. Converters are subjected to constant perturbations, such as load currents, input voltage, parameter uncertainties, switching effects and nonlinear operating points, in real-world applications. Therefore a proper control system is essential for the reliable operation of the converter, the transient response, the low ripple content and the accurate voltage regulation of the converter. Due to the ease of implementation, low computational requirement and satisfactory dynamic performance, among the various control techniques available for PE converters, the PI method is chosen. This PI controller will continuously monitor the difference between the value of the reference voltage and the actual output voltage, and generate a control voltage to minimize that difference. The integral portion of the controller is used to minimize steady state error and the proportional portion is used to speed up the response of the system by making the controller respond immediately to a change in error which causes a reduction in its rise times. The above properties ensure the PI controller is very stable and error free in many industrial and commercial applications. The tuning of the parameters of the controller is of the most important in the boost system using power electronics such as boost converter because the performance of the overall system will greatly depend on the proportional and integral gains provided in the controller. When a system is improperly tuned, it can result in excessive overshoot, oscillations, slow response, instability, longer settling time or poor disturbance rejection. Hence, various techniques to tune the controller parameters to yield a satisfactory converter performance are employed. The aim of this research is to design the PI controller to attain a regulated output voltage and improve the dynamic response and reduce the steady state error under different operating conditions[55]. In practice, conventional type PI controller can be enough to provide a good voltage regulation; however, some nonlinearities cannot be ignored during the

analysis and design of a boost converter system. Nonlinearities are found in real power electronic systems as a result of the Switching device limitations, duty cycle constraints, actuator saturation, dead zone effects, nonidealities of components and limitations of sensors. The nonlinear effects can significantly influence the converter dynamics and, in certain cases, the stability of the system, the transient response, converter ripple and converter performance. One of the significant nonlinearities which are considered in this work is saturation nonlinearity. In real (practical) converters, however, the duty cycle is limited by definite physical restrictions as the switching devices cannot function beyond a certain range. To limit the duty cycle in a safe operating range, and to avoid excessive control action and hence damage to converter components or instability, saturation nonlinearities are added. Saturation adds protection and operation safety but also brings nonlinear behaviour into the system which can impact the converter response under large perturbations and/or transient conditions. Dead-zone non-linear property is another non-linear property analysed in this work. A dead zone is an area which has a small change in the input control signal, but no corresponding change in output response. In the real world, this is often caused by the change in thresholds, the sensitivity of the actuators, or by the limits of the sensors and/or hardware. Dead zone phenomena on the controller sensitivity of boost converters can lead to slow transient response, if not considered in the system analysis. The analysis of a converter may provide a more descriptive study of the practical operating conditions by using the study of nonlinear dynamics. In the real world, all the converters have and always will be nonlinear but most conventional analyses assume a linear behavior. Therefore, the understanding of the effect of saturation and dead-zone nonlinearities will be helpful when applying the real-world limitations of converter systems and evaluating the performance of the PI controller in real world situations. The design of the PI controller of boost converter is described in detail in the following chapter and the implementation of nonlinear dynamics inside the control loop is discussed. The chapter describes the action of proportional and integral actions in voltage regulation, the importance of the correct tuning of the controller and the need for the converter to operate in a stable mode. Further, the nonlinearities of saturation and dynamics of dead zone are addressed in great detail, their practical implications are discussed, and their effect on the converter behavior is discussed. Under nonlinear operating conditions, concepts explained

in this chapter form the basis for simulation analysis and performance evaluation of closed loop boost converter. The nonlinear implementation and the controller design described here will be used in later chapters in detail in MATLAB/Simulink. Simulations, transient analysis, ripple analysis and comparison of the converter performance under various nonlinear situations.

## 5.2 Design of PI Controller for Boost Converter

Boost converter systems typically employ a PI controller for control due to its combination of simplicity, stability, and strong performance capability. The most significant requirements in the closed-loop power electronic system are to maintain an output regulated and constant voltage. In reality, many perturbations like fluctuations in the input voltage, sudden load changes, switching effects, parameter changes in components, and nonlinear operating conditions always come into effect in practical boost converter circuits. It is possible for these disturbances to result in deviations from the output voltage and a decrease in system performance if appropriate control techniques are not used. Thus, a PI controller is utilized to make sure the output voltage is regulated constantly so as to optimize the converter performance for various operating conditions.

In a closed-loop boost converter system, the PI controller continuously compares the desired reference voltage with the actual converter output voltage. The difference between these two signals is called the error signal. Based on this error, the controller generates an appropriate control action to adjust the duty cycle of the switching device. By continuously controlling the switching duty ratio. The PI controller consists of two important control actions:

- Proportional action
- Integral action

Both actions work together to improve converter performance and ensure accurate voltage regulation.

### 5.3 Proportional Action ( $K_P$ )

The proportional component of the controller is an instantaneous response to the value of the error signal. Proportional action results in a corrective control signal proportional to the size of the error as long as there is an error—that is, when the output voltage deviates from the reference voltage. This step will reduce the converter's rise time and improve its transient response to an extent.

The major functions of proportional control are:

- Improves system response speed
- Reduces rise time
- Enhances transient response
- Quickly reacts to load disturbances
- Improves dynamic performance
- Reduces output voltage deviation

A higher proportional gain generally results in faster system response and improved disturbance rejection capability. However, excessively large proportional gain may produce:

- Oscillations
- Overshoot
- Instability
- Increased ripple content

Therefore, proper selection of proportional gain is necessary to achieve stable converter operation.

## 5.4 Integral Action ( $K_i$ )

The integral part of the controller continuously accumulates the error over time and generates an additional control signal that helps eliminate steady-state error. In practical systems, small voltage errors may remain even after the transient response settles. The integral action removes these remaining errors and ensures that the output voltage reaches exactly the desired reference value.

The major functions of integral control are:

- Eliminates steady-state error
- Improves voltage regulation accuracy
- Maintains output voltage stability
- Compensates for load variations
- Enhances long-term system accuracy
- Maintains output voltage at desired reference value

Although integral action improves steady-state performance, excessive integral gain may lead to

- Slow transient response
- Increased settling time
- Oscillatory behavior
- Reduced system stability

Therefore, careful tuning of integral gain is also important for obtaining satisfactory converter performance

## 5.5 Combine effect of PI Controller

Accurate steady-state performance and quick dynamic reaction are both possible when proportional and integral control work together. While the integral action eliminates steady-state error and increases voltage regulation precision, the proportional action speeds up reaction. The overall advantages of the PI controller include:

- Simple structure
- Easy implementation
- Low computational complexity
- Stable converter operation
- Fast transient response
- Accurate voltage regulation
- Reduced steady-state error
- Improved disturbance rejection capability
- Suitable for industrial applications

Because of these advantages, PI controllers are extensively used in:

- DC-DC converters
- Renewable energy systems
- Battery charging circuits
- Electric vehicle applications
- Motor drive systems
- Industrial power supplies
- Voltage regulation systems

Proper tuning of PI controller parameters is extremely important because incorrect parameter selection may result in:

- Excessive overshoot
- Poor transient response

- Increased settling time
- Oscillations
- Instability
- Higher ripple content

Therefore, suitable tuning methods are used to determine appropriate controller gains for achieving stable operation and improved converter performance.

Overall, the PI controller provides an effective and reliable solution for controlling the output voltage of the boost converter. It improves voltage regulation capability, enhances transient response, reduces steady-state error, and ensures stable converter operation under different operating conditions.

- Proportional term ( $K_p$ ) provides an output proportional to the instantaneous error, speeding up the response & reducing the rise time of the system.
- Integral term ( $K_i$ ) accumulates the error over time, eliminating steady-state error and ensuring the output voltage settles exactly at the desired reference, even with load changes or input fluctuations.
- The PI controller output is given by:

$$u(t) = K_p \cdot e(t) + K_i \int_0^t e(t) dt$$

where  $e(t)$  is the error signal ( $V_{ref} - V_{out}$ )

## 5.6 Deriving State Space Averaging Equation

The switching action in a converter is continually cycled between ON and OFF. This has made the circuit equations also time-dependent. The direct analysis of the actual switching waveform will be very complex. To simplify this problem, a state space averaging technique is implemented to transform the switching converter into an averaged continuous time model for one switching period.

During  $0 < t < t_{on}$ , Switch is on, Diode is off.

$$-V_{in} + v_L = 0, v_L = V_{in},$$

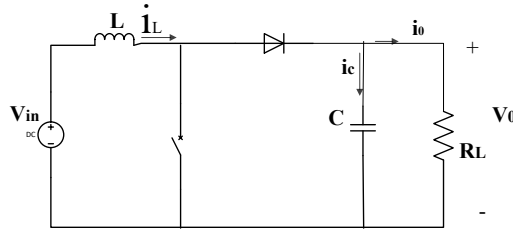


Fig5.1: Schematic diagram of a Boost Converter

$$\frac{di_L}{dt} = \frac{V_{in}}{L} \quad (5.1)$$

$$i_C + i_0 = 0;$$

$$\frac{dV_C}{dt} = -\frac{V_C}{RC} \quad (5.2)$$

During  $t_{on} < t < T$  ; switch is off and diode is on

$$-V_{in} + v_L + V_C = 0 ;$$

$$\frac{di_L}{dt} = -\frac{V_C}{L} + \frac{V_{in}}{L} \quad (5.3)$$

$$i_L = i_C + i_0 ;$$

$$\frac{dV_C}{dt} = \frac{i_L}{C} - \frac{V_C}{RC} \quad (5.4)$$

$$\text{From equation 1 and 2 we get ; } [A_1] = \begin{bmatrix} 0 & 0 \\ 0 & -\frac{1}{RC} \end{bmatrix}; [B_1] = \begin{bmatrix} \frac{1}{L} \\ 0 \end{bmatrix}$$

$$\text{From equation3 and 4 , we get } [A_2] = \begin{bmatrix} 0 & -\frac{1}{L} \\ \frac{1}{C} & -\frac{1}{RC} \end{bmatrix}; [B_2] = \begin{bmatrix} \frac{1}{L} \\ 0 \end{bmatrix}$$

$$A = A_1 \times D + A_2 \times (1 - D);$$

$$[A] = \begin{bmatrix} 0 & \frac{-(1-D)}{L} \\ \frac{(1-D)}{C} & \frac{-1}{RC} \end{bmatrix}$$

$$B = B_1 \times D + B_2 \times (1 - D);$$

$$[B] = \begin{bmatrix} \frac{1}{L} \\ 0 \end{bmatrix}$$

$$\begin{bmatrix} \frac{di_L}{dt} \\ \frac{dV_C}{dt} \end{bmatrix} = \begin{bmatrix} 0 & \frac{-(1-D)}{L} \\ \frac{(1-D)}{C} & \frac{-1}{RC} \end{bmatrix} \begin{bmatrix} i_L \\ V_C \end{bmatrix} + \begin{bmatrix} \frac{1}{L} \\ 0 \end{bmatrix} V_{in} \quad (5.5)$$

This equation 5.5 is the steady state averaging equation.

## 5.7 Deriving Small Signal Model for Boost Converter

Now To obtain linear model which is easier to analyze a small signal model has been constructed and that is linearised about steady state operating point to get required transfer functions.

Linearization is done by using the below expression

$$\begin{aligned}\hat{X} &= A\hat{x} + B\hat{u} + \{(A_1 - A_2)X + (B_1 - B_2)U\}\hat{d} \\ [A_1] - [A_2] &= \begin{bmatrix} 0 & 1 \\ -1 & 0 \end{bmatrix}; \quad [B_1] - [B_2] = 0 \\ \begin{bmatrix} L \frac{d\hat{i}_L}{dt} \\ C \frac{d\hat{v}_C}{dt} \end{bmatrix} &= \begin{bmatrix} 0 & -(1-D) \\ (1-D) & -\frac{1}{R} \end{bmatrix} \begin{bmatrix} \hat{i}_L(t) \\ \hat{v}_C(t) \end{bmatrix} + \begin{bmatrix} 1 \\ 0 \end{bmatrix} \begin{bmatrix} \hat{V}_{in} \\ 0 \end{bmatrix} \begin{bmatrix} V \\ -I \end{bmatrix} \hat{d}\end{aligned}\quad (5.6)$$

On solving above equation (5.6) using Laplace and inverse Laplace transforms and making  $\widehat{V}_{in}(s)$  is equal to zero one can get the transfer function between control input 'd' to output voltage 'V' is given as equation

$$\frac{\widehat{v}_S(s)}{\hat{d}(s)} = \frac{\frac{V_{in} - I_L s}{LC} \frac{I_L s}{C}}{s^2 + \frac{1}{RC}s + \frac{(1-D)^2}{LC}} \quad (5.7)$$

This equation 5.7 is transfer equation of Boost Converter

## 5.3 Finding $K_p$ and $K_i$ value for PI Controller

Here, it is assumed that  $L_r$  and  $C_r$  are not present.

Transfer function of boost converter

$$G(s) = \frac{\frac{V_{in} - I_L s}{LC} \frac{I_L s}{C}}{s^2 + \frac{1}{RC}s + \frac{(1-D)^2}{LC}} \quad [11]$$

Transfer function of PI controller

$$G_C(s) = G_\infty \left(1 - \frac{w_L}{s}\right) \quad [11]$$

$$w_c = \frac{w_{sw}}{20} = 2.5kHz$$

$$w_L = \frac{w_c}{10} = 250Hz$$

$$G_{\infty} = \frac{\sqrt{\left(\frac{(1-D)^2}{LC} - \omega_c^2\right)^2 + \left(\frac{1}{RC}\right)^2}}{\sqrt{\left(\frac{V_{in}}{LC}\right)^2 + \left(\frac{I_L \omega_c}{c}\right)^2} \sqrt{1 + \left(\frac{\omega_L}{\omega_c}\right)^2}}$$

$$K_p = G_{\infty} = 0.032$$

$$K_i = G_{\infty} \times \omega_L = 4.9475$$

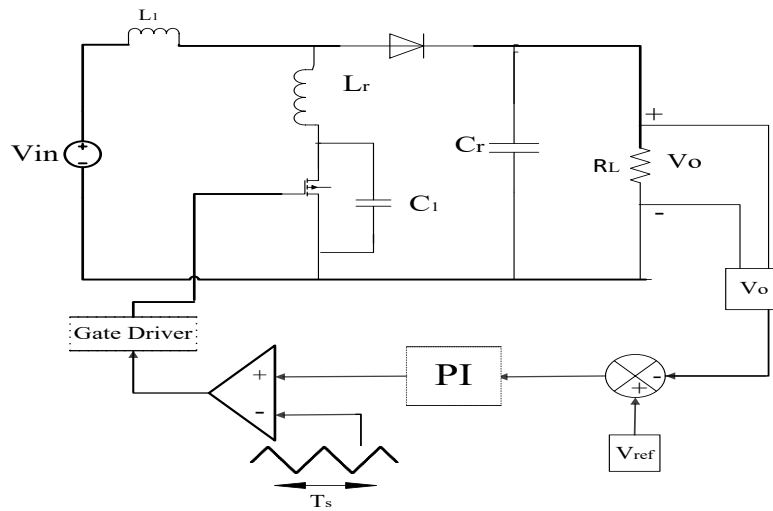


Fig5.2: Simulation of ZVS Boost converter using PI

## CHAPTER 6

### TYPES OF ZVS BOOST CONVERTER

#### 6.1 M-type Half-wave ZVS Boost Converter

A family of ZVS quasi resonant converter is shown in Fig8 and Fig10. These converters are obtain by adding a resonant capacitor  $C_r$  in parallel with the switch and the resonant inductor  $L_r$  in series with parallel combination of the switch and the resonant capacitor in the conventional pwm converters.

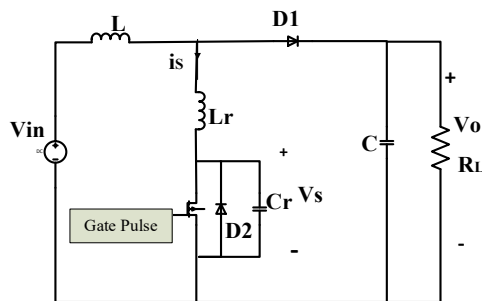


Fig6.1 : Schematic diagram for M-type Halfwave Boost Converter

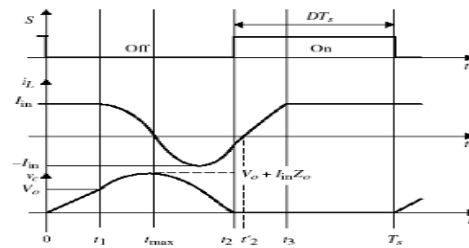


Fig6.2: Steady state wave from M-type Half-wave Boost Converter [11]

From Fig9 when switch and diode  $D_1$  both are off, the resonant inductor current  $i_{Lr}$  start increasing linearly and resonant capacitor is also getting charge by constant source current ,voltage  $V_{Cr}$  start increasing linearly. At time  $t = t_1$ , inductor current get maximum upto source current  $I_{in}$  and resonant capacitor voltage  $V_{Cr}$  is upto output voltage  $V_0$ , then switch is off and diode  $D_1$  is on. Now  $C_r$ - $L_r$ - $V_0$  forms a resonating path ,Resonant inductor current equation is like

$$i_{Lr}(t) = I_{in} \cos w_0(t - t_2). \text{ Resonant capacitor voltage } V_{Cr}(t) = V_0 + I_{in}Z_0 \sin w_0(t - t_1).$$

At  $t=t_{max}$  ,  $i_{Lr}(t) = 0$  and  $V_{Cr}(t)$  is maximum i.e  $(V_0 + I_{in}Z_0)$  Volt.

At  $t = t_2$ ,  $V_{Cr}(t)=0$  , current passing through body diode  $D_2$ . After  $t_2$ , we can on the switch. So across the switch, voltage is zero and switch current start linearly increasing. After  $t=t_3$ , switch current reaches maximum and diode  $D_1$  will be off.

### 6.2 M-type Full-wave ZVS Boost Converter

This type of converter only allow one direction of current flow but the direction of voltage is bi-directional.

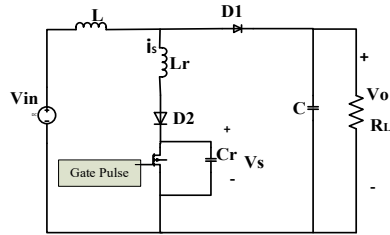


Fig6.3: Circuit diagram of M-type Full-wave ZVS Boost Converter

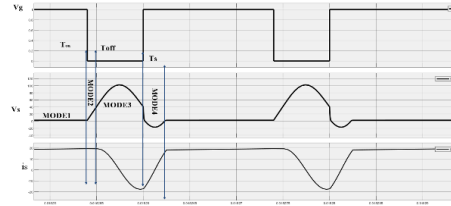


Fig6.4: Steady state waveform of M-type Full-wave ZVS Boost Converter

From the above figure when switch is on and diode D1 is off, inductor is storing charge. Now switch is off and diode D1 is also off, at this time Cr(resonant capacitor) starts storing charge. When Vcr will be equal to Vo(output voltage) then diode D1 will be on and inductor current starts decreasing with a cosine function. When inductor current is it's -ve peak  $I_{in}$  then Vcr(resonant capacitor voltage) is zero. When switch and diode D1 both are on, inductor start charging again, it try to reach  $I_{in}$  from  $-I_{in}$ . Vcr goes to -ve and it comes again zero when inductor current touches at zero.

### 6.3 L-type Half-wave ZVS Boost Converter

L-type refers to the shape and configuration of the resonant auxiliary circuit in an L-type Half-Wave ZVS Boost Converter, particularly the connection of the inductor (L) with the switch and resonant elements.

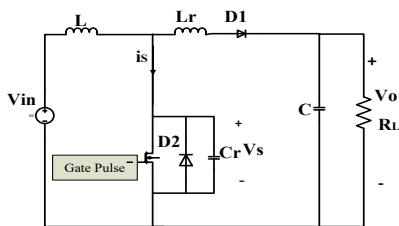


Fig6.5: Circuit diagram of L-type Half wave ZVS Boost Converter

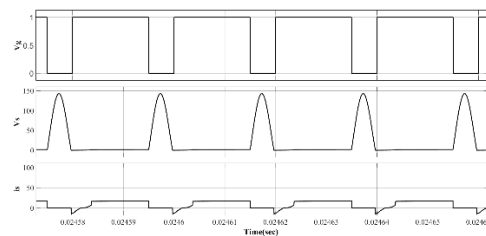


Fig6.6: Steady state waveform of M-type Full-wave ZVS Boost Converter

When switch and diode D1 both are off, Then resonant capacitor start charging by constant current source. When diode D1 is on then resonant capacitor, resonant inductor and load from a resonating path. This resonating path helps the voltage across the switch become zero although current through the switch is not zero completely.

## 6.4 L-type Full-wave ZVS Boost Converter

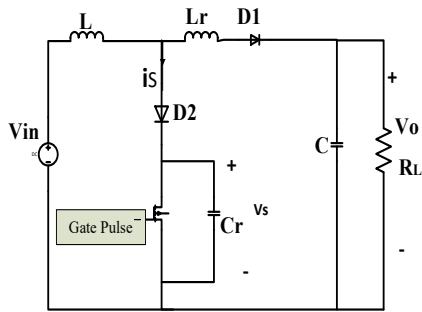


Fig6.7: Circuit diagram of L-type Full-wave ZVS Boost Converter

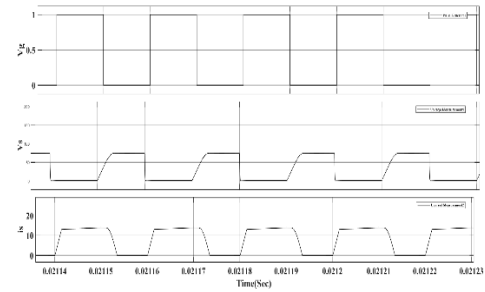


Fig6.8: Steady state wavefrom of L-type Full wave ZVS Boost Converter

From the figure it's shows that when diode is connected series with the switch it blocking -ve current but it allows bi-directional of voltage. when switch is on , resonant capacitor voltage is zero and when it off resonant capacitor start getting charge. When it is reached equal to output voltage  $V_o$ , then diode D1 is on and it is in the resonating cituation. From the figure current flowing through the switch is 21.6 A and voltage across the switch is 80V, it is a peak voltage

## CHAPTER 7

### DESCRIPTION OF THE ZCS BOOST CONVERTER & OPERATING PRINCIPAL

#### 7.1 Overview

ZCS Boost converter circuit are obtained by adding a resonant inductor  $L_r$  in series with the transistor and a resonant capacitor  $C_r$  in parallel with the series combination of the switch and the resonant inductor  $L_r$ . When power MOSFET with its body diode then it behave as a bi-direction switch for current and uni-direction for voltage. It's circuit is called as full wave ZCS converter. If a diode is added with series with MOSFET then it is called half wave ZCS converter. Family of ZCS Boost Converter are shown in the Fig7.1 and Fig7.3 .

#### 7.2 Half-wave ZCS Boost Converter operating principal

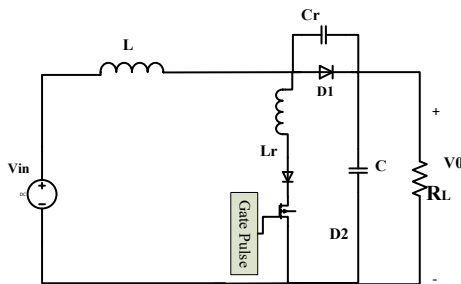


Fig7.1:Circuit diagram of Half-Wave ZCS Boost Converter

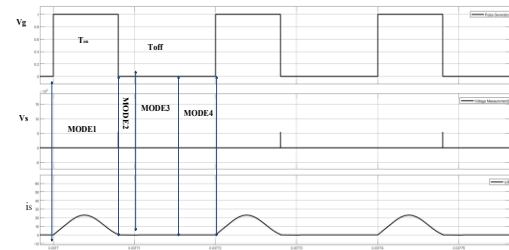


Fig7.2 :Steady state wavefrom of Halfwave ZCS Boost Converter

From the above figure Assume Switch is on, initially inductor current and capacitor voltage are zero. When the resonant inductor current reaches the input current  $I_{in}$  , the diode turns off. Converter enters mode 2. At mode2 the switch remain closed ,but the diode is off at mode2. This is a resonating mode during which capacitor voltage starts decreasing from its initial value of  $V_0$ . When inductor current reaches  $I_{in}$  current then capacitor reaches its negative peak. When inductor current equals zero, and the switch turn off. Mode3 switch and diode both are open. Since capacitor voltage is constant, the capacitor starts charging up by the input current source. At mode4 the capacitor voltage is clamped to the output voltage, and diode starts conducting again. The cycle of mode repeat again at the time of  $T_s$  when Switch S is turned on again.

### 7.3 Full-wave ZCS Boost Converter operating principal

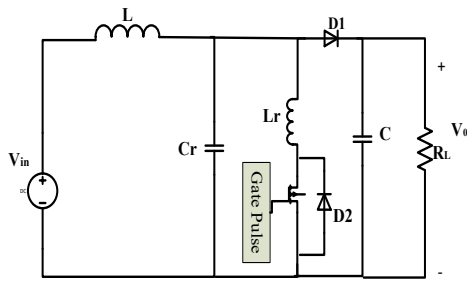


Fig 7.3: Circuit diagram of Full-wave ZCS Boost Converter.

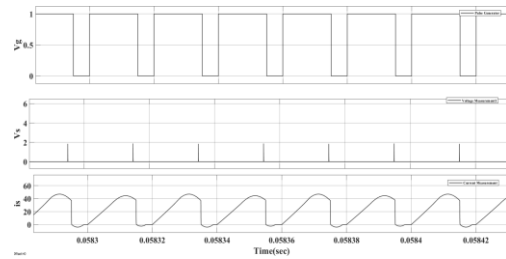


Fig 7.4: Steady-state waveform of Full-wave Boost Converter

From the figure, assume switch and the diode both are on. Initial resonating inductor current was zero and initial resonant capacitor voltage was output voltage  $V_0$ . Inductor current reaches upto input source current. When inductor current reaches upto input source current then diode D1 will turn off. The switch and diode remain off, this is a resonating mode during which capacitor voltage starts decreasing resonantly from its initial value of  $V_0$ . When inductor current will zero after some time then at that point capacitor voltage will reaches -ve peak. When switch and diode both are open capacitor charging up by the input current source. When capacitor voltage again charge upto output voltage then diode begins conducting.

This mode of cycle will repeat again at the time of  $T_s$  when switch S is turned on again. From this graph switch current is bi-directional and switch voltage is uni-directional. When switch is off, the switch current is zero but switch voltage may not be zero.

## CHAPTER 8

### RESULT & DISCUSSION

#### 8.1 ZVS-Boost Converter performance in open loop

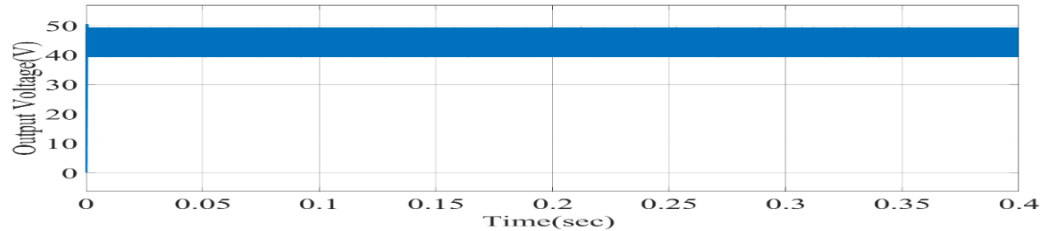


Fig8.1a: ZVS-Boost Converter output voltage in open loop

From Fig 8.1a, it is showed that at time  $t = 0.3$  msec, output voltage of the ZVS boost converter reaches to steady state value and voltage ripple is about to 4.95V due to the resonant component in the converter. By connecting high value of capacitor at load end will reduce the ripple drastically

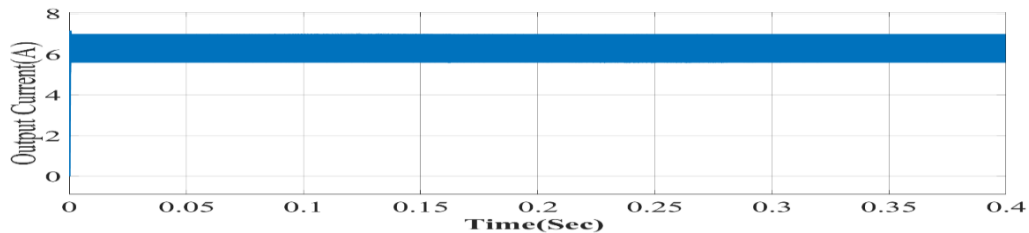


Fig8.1b: ZVS-Boost Converter output current in open loop

Fig 8.1b shows that at time  $t = 0.3$  msec, output current of the converter reaches at steady state and because of resistive load is used, output current follows output voltage and current ripple is about to 1.5A. Further output voltage and current are coming as 46.25V and 7.53 A respectively

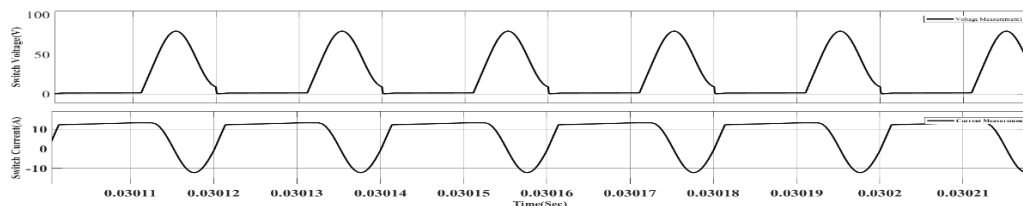


Fig8.1c: ZVS-Boost Converter switch current and switching voltage in open loop

From Fig:8.1c,It also shows that in the converter switch ZVS and ZCS are occurred simuntaneously.

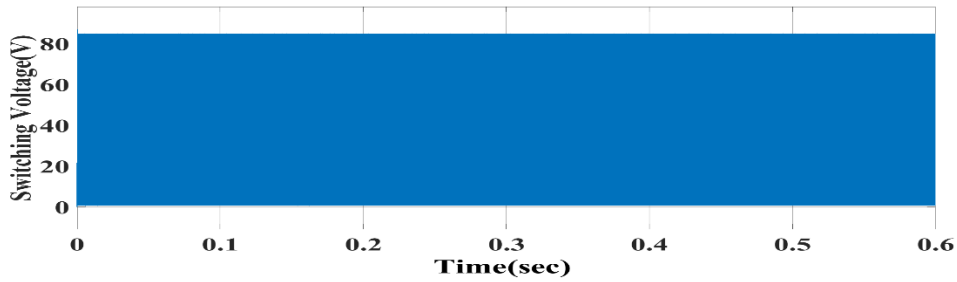


Fig 8.1d: Voltage across the switch in open loop

From Fig:8.1d, voltage across switch is 1.7 times of output voltage. After 0.3msec, maximum switch voltage is 82.32V and minimum switch voltage is 1.5V .

## 8.2 Load Regulation of ZVS Boost Converter in open loop

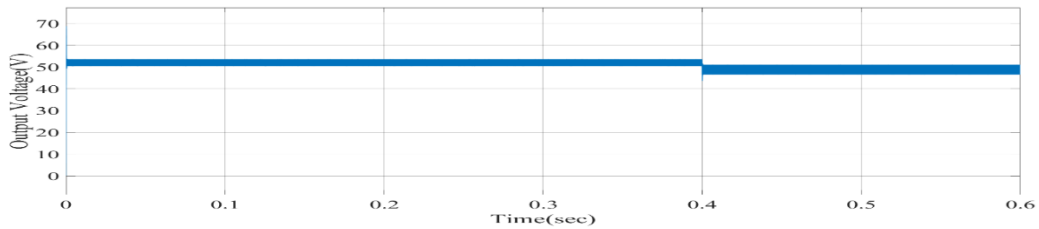


Fig8.2a: Output voltage of ZVS Boost Converter during Load -Regulation

From Fig8.2a, upto time  $t=0.4\text{sec}$  average output voltage is 56.8V and after that average output voltage is 52.21V. It is because of loading from  $50\Omega$  to  $50\Omega||100\Omega$ .

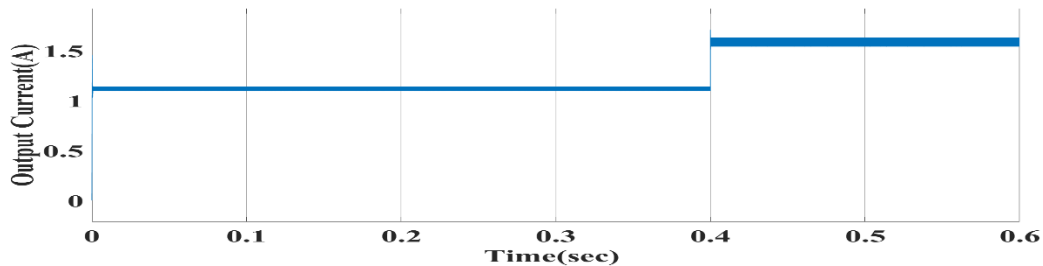


Fig8.2b: Output current of ZVS Boost Converter during Load -Regulation

From Fig8.2b, it is seen that upto  $t=0.4\text{sec}$ , average output current is 1.24A and after that it is 1.62A because of high loading and equivalent resistance come down from  $50\Omega$  to  $37.5\Omega$ .

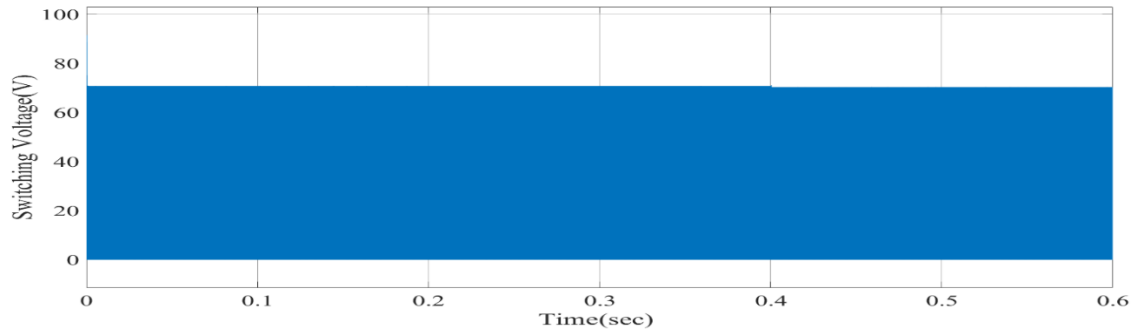


Fig8.2c: Switching voltage of ZVS Boost Converter during Load -Regulation

From Fig13, it is seen that upto  $t=0.4$  sec, voltage across switch is 73.6V and after 0.4sec, voltage is around 62.2V.

### 8.3 ZVS Boost Converter performance using PI controller

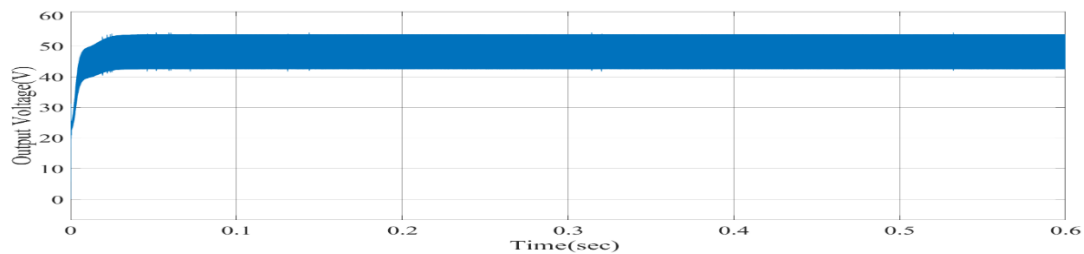


Fig8.3a: Output Voltage of Boost Converter using PI Controller

From Fig8.3a, output voltage is varied from 43.31V to 52 V. Using PI controller, average output voltage of the converter is improved.

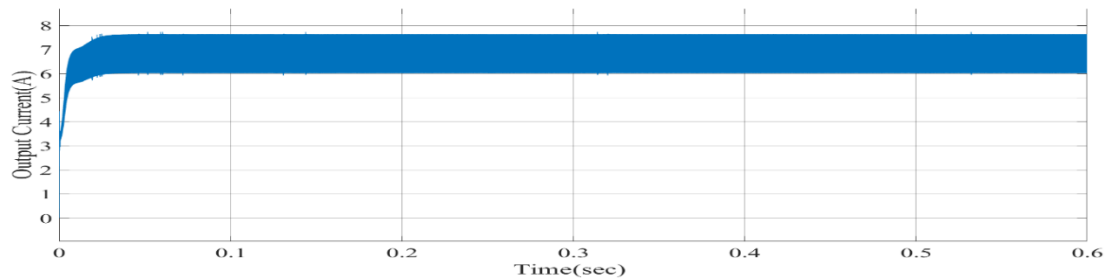


Fig8.3b: Output Current of Boost Converter using PI Controller

From Fig15, it is seen that load current follows the output voltage waveform. Moreover, load current is varied from 5.8A to 7.7A. Using PI controller, the load current is not much affected and nearly of same value. Thus there is need of current loop and can be implemented in future studies

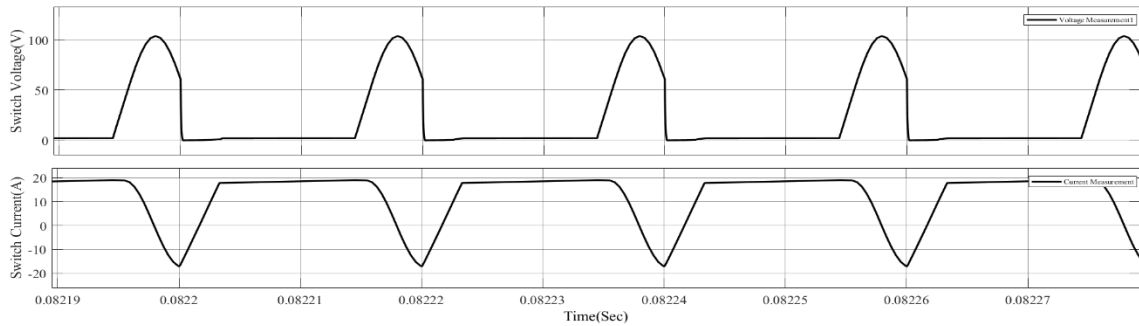


Fig8.3c: Switching current & Switching voltage of Boost Converter using PI Controller

From Fig8.3c. It shows that during use of PI controller converter's switch performs ZVS and ZCS simultaneously.

#### 8.4 Load Regulation of ZVS Boost Converter using PI Controller

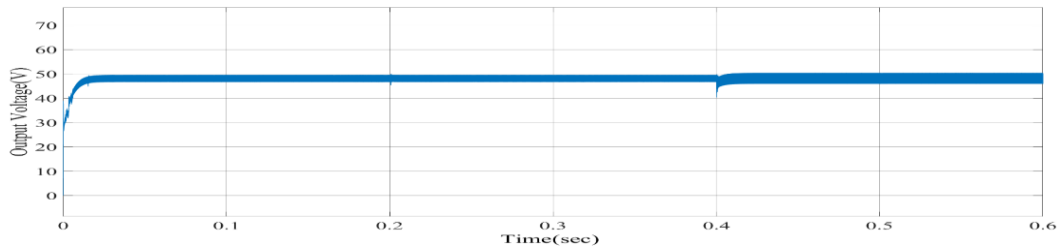


Fig8.4a: Output voltage of Boost Converter during Load-Regulation using PI Controller

From the Fig8.4a it is seen that output voltage remain same even though, at  $t=0.4$  sec load is increased. Average output voltage through out is 47.25V and voltage ripple is 2.35V.

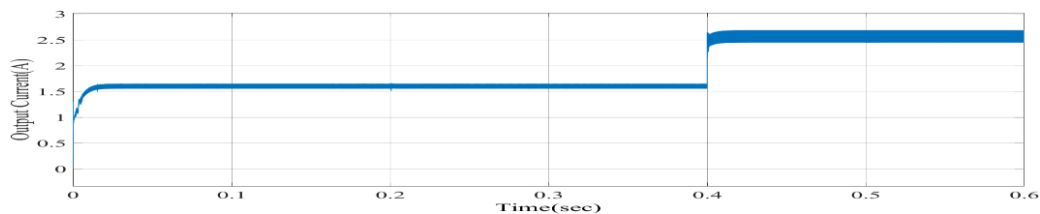


Fig8.5b :Output current of PI Controller based ZVS Boost converter during varying load

From Fig8.5b, it is seen that upto 0.4 sec output current is 0.9A when load is increased the output current is also increased as 1.42A

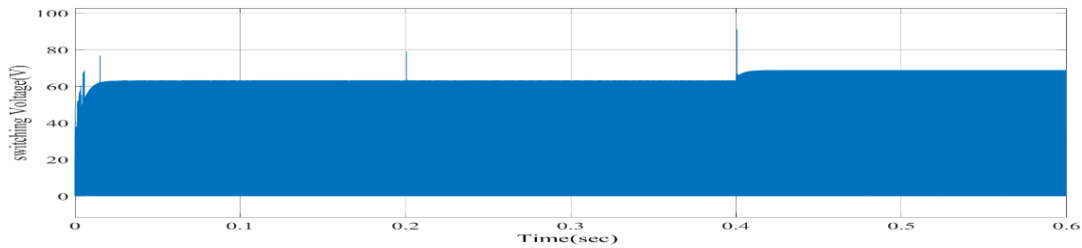


Fig8.5c: Switching voltage of Boost Converter during Load-Regulation using PI Controller

From Fig 8.5c, it is seen that upto 0.4 sec, voltage across the switch is 58.84V and after this it is 62.56V.

### 8.5 Compared results of different ZVS Switching schemes

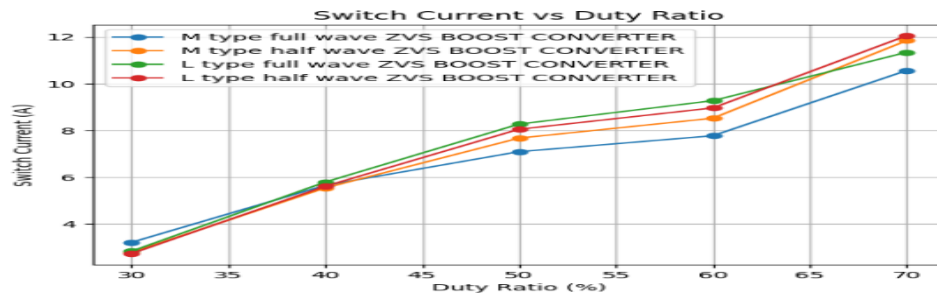


Fig8.5a: Switching current compare graph between M-type Full wave, Half-wave, L type Full-wave, Half-wave ZVS Boost converter

From the above graph L-type Half-wave ZVS Boost converter has highest switching current nearly 12A. In 30% duty ratio the switch currents of M-type Full-wave, Half -wave and L-type Full-wave, Half -wave ZVS Boost converter are 2.786A, 3.21A, 2.73A and 2.83A respectively. In 50% duty ratio the switch currents of M-type Full-wave, Half -wave and L-type Full-wave, Half -wave ZVS Boost converter are 7.678A, 7.09A, 8.05A and 8.27A respectively. In 70% duty ratio the switch currents of M-type Full-wave, Half -wave and L-type Full-wave, Half -wave ZVS Boost converter are 11.84A, 10.56A, 12.05 and 11.3aA respectively

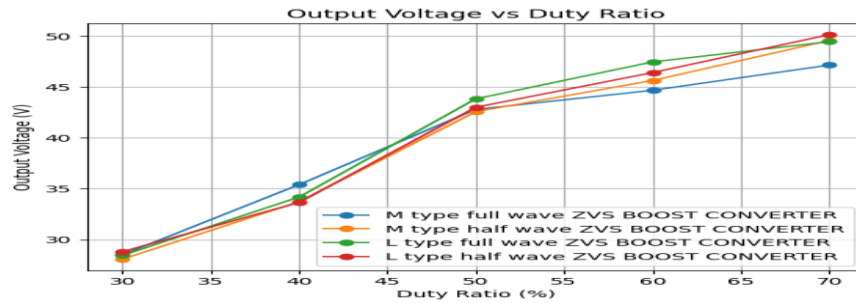


Fig8.5b: Output voltage compare graph between Full wave, Half wave M-type L-type ZVS Boost converter

From the duty varies 30-70% output voltage of Full-wave M-type ZVS Boost converter output voltage vary from 28.8V to 47.8V and Half wave M-type ZVS Boost converter vary from 26.2V to 45.8V and L-type Full-wave ZVS Boost converter's output voltage vary from 28.08V to 50.15V and L-type Half-wave ZVS Boost converter's output voltage vary from 28.44V to 49.46V.

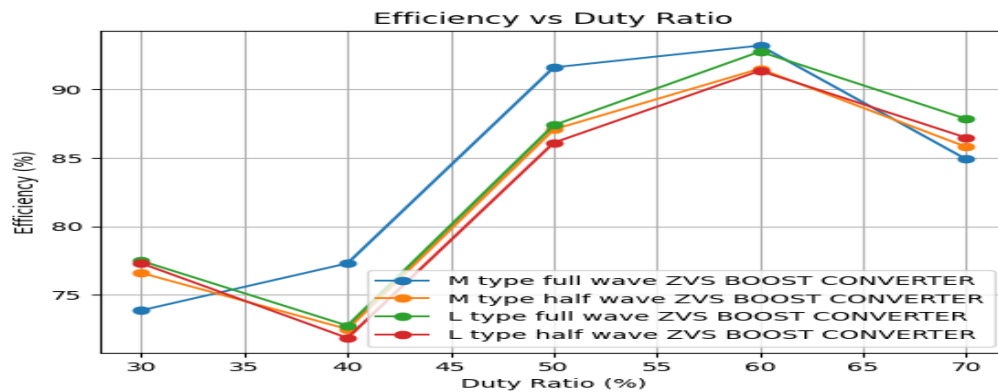


Fig8.5c: Efficiencies compare graph between Full wave, Half wave M-type, L-type ZVS Boost converter

From the above graph it is seen that we get maximum efficiency at duty is equal to 60%. At 30% duty ratio M-type Full-wave ZVS boost converter shows 76.6% efficiency, M-type Half-wave ZVS Boost converter shows 73.83% efficiency and L-type Full-wave ZVS boost converter show 72.3% and L-type Half-wave ZVS Boost converter show 77.48% efficiency. At duty 60% M-type Full -wave ZVS Boost converter shows 93.19% efficiency.

## 8.6 Switching Current comparison between ZVS & ZCS Boost Converter

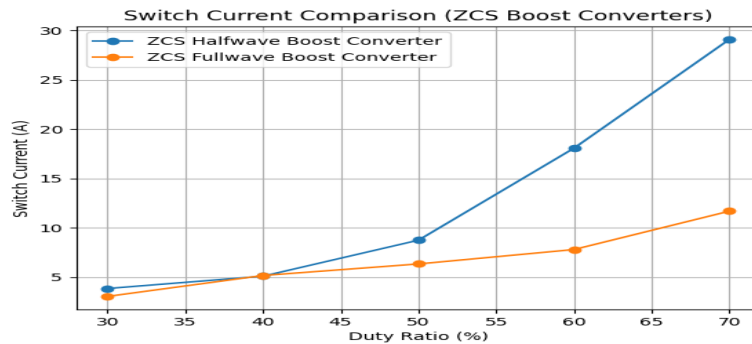


Fig8.6: Switching current compare graph between ZCS Full-wave and ZCS Half-wave Boost converter

From the above at duty 70%, the switch current of ZCS full wave Boost Converter and ZCS half wave Boost Converter are 12.3A,28.24A respectively. At duty 50%, the switch current of ZCS full wave Boost Converter and ZCS half wave Boost Converter are 6.33A,21.18A respectively.

## 8.7 Switching Voltage comparison between ZVS & ZCS Boost Converter

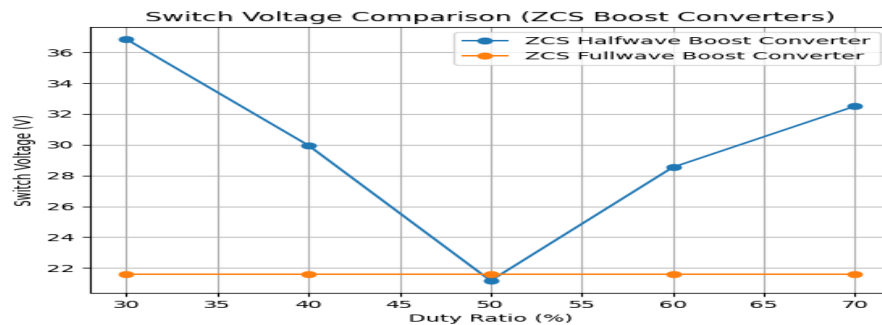


Fig8.7: Switching voltage compare graph between ZCS Full-wave and ZCS Half-wave Boost converter

From the above Voltage across the switch of ZCS Full-wave Boost Converter is same 21.6V, but in case of ZCS Half-wave Boost converter, at duty 30% voltage stress across the switch is maximum i.e 38V. At 70% duty the voltage stress across switch of Half-wave ZCS Boost converter is 33.1V, At 50% duty the voltage stress across switch is 21.2V.

## 8.8 SIMULATION BASED RESULT

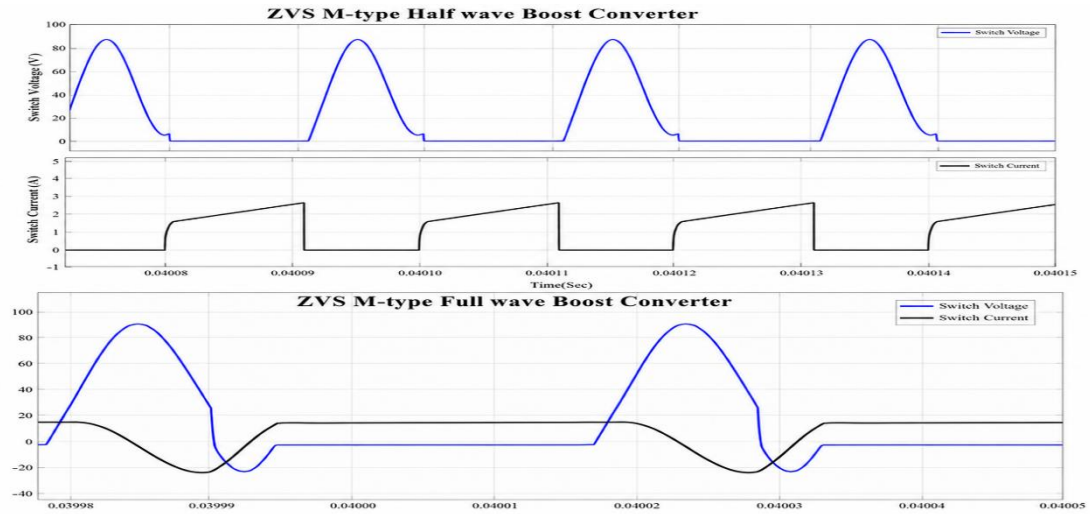


Fig8.8a: Comparison switching stress and switching current in between ZVS M-type Full-wave & Half wave Boost converter

From the graph At 50% duty ratio maximum switching voltage is 43.67V and switching current is 12.12A.

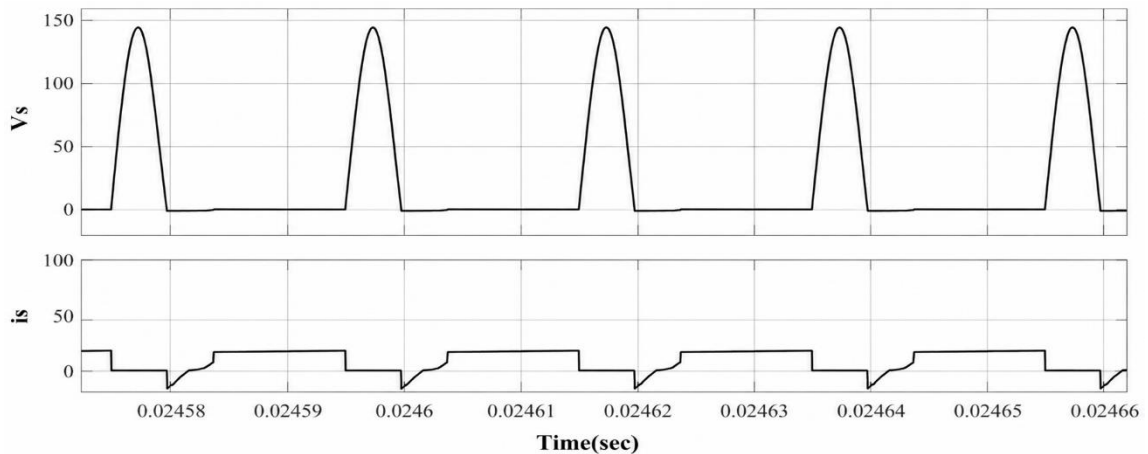


Fig8.8b: Voltage stress and switching current of ZVS L-type Half wave Boost Converter

Above graph is obtained when we were taking duty ratio is equal to 50%. Voltage stress of switch is equal for both half/full wave converter but switching current wave are different.

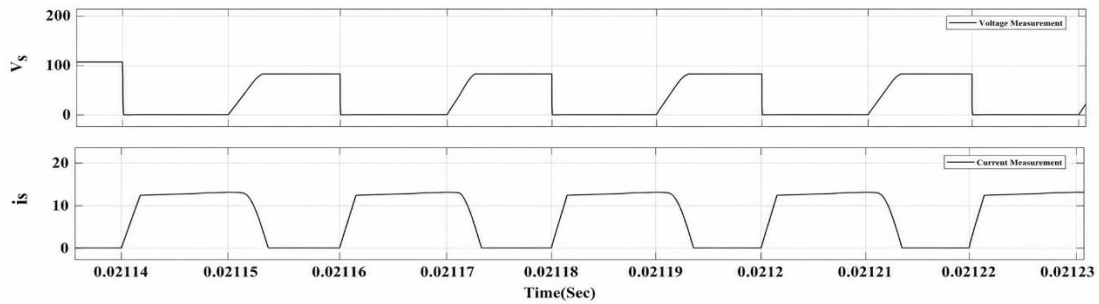


Fig8.8c: Voltage stress and switching current of ZVS L-type Full- wave Boost Converter

Above graph is obtained when we were taking duty ratio is equal to 50%. Voltage stress of switch is equal for both half/full wave converter but switching current wave are different.

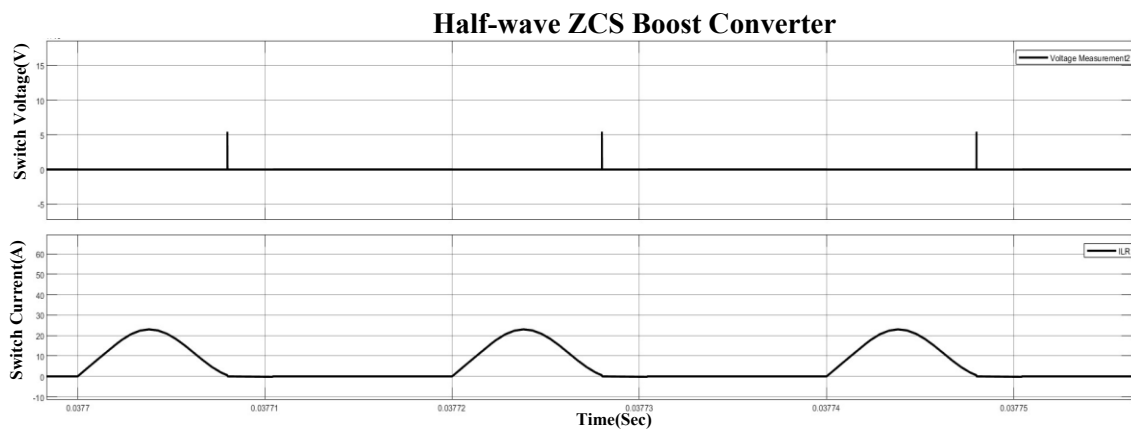


Fig8.8d: Voltage stress & switching current of Half-wave ZCS Boost converter

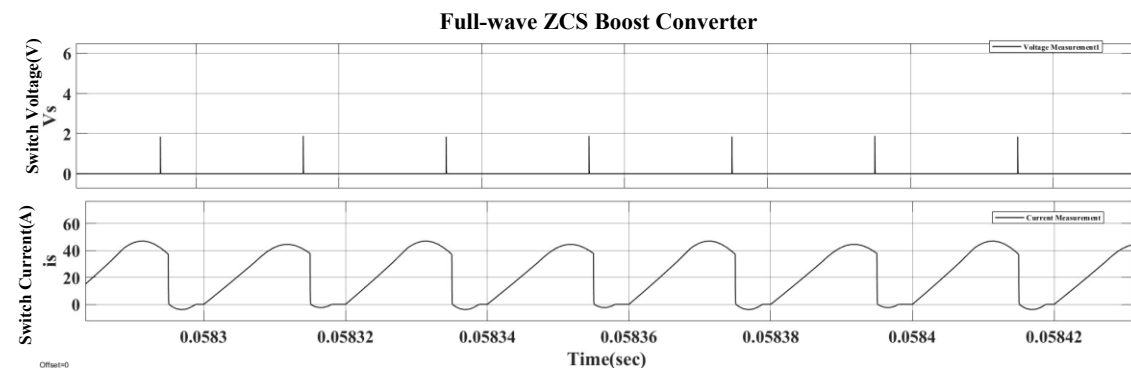


Fig8.8e: Voltage stress & switching current of Full-wave ZCS Boost converter

From Fig:8.8d &8.8e, we may conclude that from switching stress point of Half-wave ZCS Boost converter is more superior than Full-wave ZCS converters.

## 8.9 Discussion

From 8.5 to 8.7 , All compared results are made by taking below parameters

Input Voltage(V)	21.6
Filter Inductor( $\mu$ H)	180
Switching Frequency(kHz)	50
Resonant Inductor( $\mu$ H)	5
Resonant Capacitor( $\mu$ F)	0.5
Filter Capacitor ( $\mu$ F)	8
Load Resistance( $\Omega$ )	7

Table2: Parameters are considered for Converters

From the above discussion we may conclude in case of ZVS point of view M-type half wave Boost Converter has better efficiency than other type of ZVS Boost Converter (considering all ZVS converters are operating in 50% duty). Switching stress of all ZVS converters are nearly same i.e nearly 100V but current passing through switch is more in L type of ZVS converters. Full-wave ZCS Boost Converter has better efficiency and current flow through the switch is lesser than half-wave ZCS converter but switching stress is comparatively more.

ZVS Boost Converter is designed and controlled via PI controller in the present work. It was found that switch voltage is reduced due to ZVS action. Further it may reduce the junction temperature causing less failure rate of MOSFET as a switch. PI controller work Properly through for less ranges of load during ZVS operation. By seeing voltage waveform across the switch during ZVS operation, voltage comes at zero after every cycle. If we will increased L and C value by keeping Kp and Ki value constant then output voltage shown very little voltage variation.

# CHAPTER 9

## CONCLUSION & FUTURE SCOPE

### 9.1 Conclusion

The present research work was directed towards the Design, Modeling, Analysis and Control of a Zero Voltage Switching (ZVS) Boost Converter by implementing a PI controller for better performance of the converter under varying operating conditions. The proposed converter was designed to reduce switching losses, to minimize voltage stress across the switch and to enhance the overall converter efficiency, particularly for renewable energy system applications and electric vehicle applications where an efficient DC-DC converter is critical. The voltage and current overlap during switching transition in conventional PWM boost converter, which results in high switching losses, increased electromagnetic interference and higher device stress. To overcome these problems, one of the soft switching ZVS technique was implemented in the proposed converter. This method has a very small switching voltage (close to zero), which results in fewer switching losses and less stress on the MOSFET. Soft switching operation was successfully achieved by using the resonant inductor and resonant capacitor in the converter topology. It was explained how the converter works in the various operating modes and each mode explained the operation of the switch, diode, resonant components and load on the switching cycle. The vibration effect enabled the switch voltage to go close to zero before turn-on, which proved the switch functions correctly in the ZVS mode. Successful mathematical modelling and design analysis of the converter was also completed. The converter input voltage is 21.6V and output voltage is 48V and switching frequency is 50kHz. The values of the resonant inductor, resonant capacitor, filter inductor and filter capacitor have been carefully calculated to obtain the desired performance of the converter. In the first step, the open loop performance of the ZVS boost converter was studied using MATLAB simulation in R2023a. The results indicate that the steady-state

output voltage was achieved rapidly and the converter was able to increase the voltage to the desired value. However, some voltage and current ripples were noticed due to resonance operation. The voltage across the switch verified that switch voltage dropped considerably after ZVS operation, which helped to minimize switching losses and enhance the converter reliability. By analyzing load regulation in the open-looped condition, it was found that the output voltage changed as the load conditions changed, so a control system to achieve stable output voltage was necessary. Thus, a PI controller was designed and implemented in closed loop system. Proper tuning of proportional and integral gains was done to enhance transient response and voltage regulation capability. The simulation results under closed loop control indicated that output voltage was kept near to the reference voltage (48V) even in the presence of load variation when the PI controller was used. The output voltage ripple was significantly decreased, and the converter showed improved stability and robustness than the open-loop systems. The output current was also correctly modulated in response to the voltage and the current variation was within the limits. In addition, with the use of the PI controller, the voltage stress across the switch was further reduced, further demonstrating the effectiveness of the proposed control method. The simulation results showed that the ZVS boost converter with the proposed PI control approach could work properly under different load configurations, and that the output voltage was kept stable and the switching stress was reduced. The proposed converter also has benefits like less on switching losses, less EMI, more efficient, less junction temperature, and more reliable semiconductor devices. From the comparative study of earlier works, it was observed that most of them were studied in an open loop condition while in the proposed work, the closed loop operation of the ZVS converter was successfully demonstrated using PI controller. Therefore, the present work aims at achieving the better voltage regulation and stable operation of ZVS boost converter in real-time applications. Based on the study, the proposed PI controlled ZVS boost converter is found to be the efficient, reliable and effective solution for modern power electronic applications with particular reference to renewable energy and electric vehicle and high frequency DC-DC conversion system. For further enhancement of the converter performance, future work can be done on efficiency optimization, advanced control

techniques, current loop control and intelligent controllers under practical operating conditions in hardware implementation.

## 9.2 Future scope

Future work can involve experimental testing and validation of the proposed PI controlled ZVS Boost Converter under practical operating conditions with hardware implementation. Advanced control laws like PID, fuzzy logic, sliding mode, adaptive and neural network controllers can be used to enhance dynamic response and stability. A current control loop can also be included to ensure more accurate control and protection. Resonant components can be further optimized to further reduce the voltage and current ripple. The converter extends to renewable energy systems, PV applications, battery charging systems, DC microgrids and electric vehicle applications. SiC and GaN devices can also be utilized for high-frequency operation to enhance the efficiency and power density of the devices. Industrial Applications: Thermal analysis, EMI reduction and reliability studies are possible. In the future, comparative analysis with other soft-switching converters such as ZCS can be conducted.

For finding  $K_p$  and  $K_i$  one assumption has taken that resonant inductor and resonant capacitor were absent i.e converter be like 2<sup>nd</sup> order, that is why  $K_p$  and  $K_i$  value were not accurate.

## REFERENCES

- [1] K. Liu and F. C. Lee, " Zero-voltage switching technique in dc/dc converters," IEEE Power Electronics Specialist Conference Record, pp :58-70, 1986.
- [2] M. K. Kazimierczuk and J. J'ó'zwick, "New topologies of high-efficiency high-frequency zero-voltage switching resonant dc/dc converters.," Proc. 29th IEEE Midwest Symposium on Circuits NE, pp: 474–477, 1986.
- [3] P. C. Todd and R. W. Lutz, " Practical resonant power converters – Theory and applications.," in IEEE, Powertechnique Magazine, pp:29–35, May 1986.
- [4] M. K. Kazimierczuk and J. J'ó'zwick, " Analysis and design of buck zero-voltage-switching resonant dc/dc converter.," Proc. 12th International PCI'86 Conference, Boston, MA, pp:35–54,1986.
- [5] M.K.Kazimierczuk, W. D. Morse, "State-plane analysis of zero-voltage-switching resonant DC/DC converter," in IEEE Transactions on Aerospace and Electronic Systems, vol. 25, pp: 232–239,, 1989.
- [6] M. K. Kazimierczuk, " Design-oriented analysis of boost zero-voltage-switching resonant DC/DC converter," IEEE Transactions on Power Electronics, vol. 3, no. 2, pp: 126–135, April 1988.
- [7] B.R.Lin and. Fang-Yu-Hsieh, "Soft-switching zeta-flyback converter with a buck-boost type of active clamp," IEEE Transactions on Industrial Electronics, vol. 54, no. 5, pp:2813–2822, 2008.
- [8] P. S. Shandilya, Ashutosh, D. Joshi and N. Kumar, "Modelling of PID-based Closed-Loop Voltage Mode Control for Cuk Converter with Circuit Parasitics," IEEE 4th International Conference on Sustainable Energy and Future Electric Transportation (SEFET)," pp:1-5,2024
- [9] P.Usha, Priyanka K ""Design and Implementation of Closed Loop Soft Switching Boost Converter using PI Controller",," in IEEE, Volume 6 Issue 5 , International Journal on Recent and Innovation Trends in Computing and Communication (IJRITCC), ISSN: 2321-8169, APA pp: 253 -261,May 2018.
- [10] Dheeraj Joshi,Sudha Bansal,Lalit Mohan Saini "Design of a DC DC converter for photovoltaic solar system", in IEEE 5th India International Conference on Power Electronics (IICPE), pp :1-5, December 2012.

- [11] Robert W Erickson. & Dragan Maksimovic. "Fundamentals of Power Electronics" ,2nd edition. pp: 331-369,May1989.
- [12] Genesia C Tavares,Noah Dias, "Analysis and Design of A Zero Voltage Transition DC-DC Boost Converter," International Journal of Engineering Research and Technology (IJERT) ISSN:2278-0181,vol.11, pp:1-9, July-2022.
- [12] Souhali Barakat, Badr N'Hili, Addelouahed Mesbani, Karim-Et-Torabi, "ZVS QR boost converter with variable input voltage and load," in 3rd International Conference on Innovative Research in Applied Science, Engineering and Technology (IRASET), pp:1-6 May-2023.
- [13] Arijit Nath,Dheeraj Joshi " "Design and Control of PI Controller Based ZVS Boost Converter," 2025 IEEE DELCON - International Conference on Recent Smart Technologies in Engineering for Sustainable Development, New Delhi, India, pp. 1-8, 2025 doi: 10.1109/DELCON68055.2025.11400146.
- [14] M. J. Baig and R. K. Singh, "A Soft-Switched ZVS-ZCS Boost Converter Design and Analysis," 2024 IEEE 3rd International Conference on Electrical Power and Energy Systems (ICEPES), Bhopal, India, pp. 1-4, 2024 doi: 10.1109/ICEPES60647.2024.10653601.
- [15] M. R. Yazdani and M. Pahalvandust, "A Single-Switch ZCS Boost Converter with Low Conducted EMI," 2019 International Aegean Conference on Electrical Machines and Power Electronics (ACEMP) & 2019 International Conference on Optimization of Electrical and Electronic Equipment (OPTIM), Istanbul, Turkey, pp. 336-340, 2019, doi: 10.1109/ACEMP-OPTIM44294.2019.9007224.
- [16] S. Sooksatra and W. Subsingha, "Analysis of Quasi-resonant ZCS Boost Converter using State-plane Diagram," 2020 8th International Electrical Engineering Congress (iEECON), Chiang Mai, Thailand, pp.1-4,2020 doi: 10.1109/iEECON48109.2020.229543.
- [17] M. T. Kuriyakose and A. Rajan, "Closed loop control of ZCS interleaved high step up converter for sustainable energy applications," 2016 International Conference on Electrical, Electronics, and Optimization Techniques (ICEEOT), Chennai, India, 2016, pp. 990-995, doi: 10.1109/ICEEOT.2016.7754834

## List of Publications

1. Arijit Nath, Dheeraj Joshi " "Design and Control of PI Controller Based ZVS Boost Converter," 2025 IEEE DELCON - International Conference on Recent Smart Technologies in Engineering for Sustainable Development, New Delhi, India, pp. 1-8, 2025 doi: 10.1109/DELCON68055.2025.11400146. (PUBLISHED)



2. Arijit Nath , Prof Dheeraj Joshi “” Performance analysis of Boost Converter using softswitching schemes”” in the Fifth edition of the International Conference on Emerging Frontiers in Electrical and Electronic Technologies (ICEFEET-2026) is being organised at the Department of Electrical Engineering, NIT Patna on 09-10, July 2026. **(ACCEPTED)**

Dear Dheeraj Joshi,

The organizing team of the Department of Electrical Engineering, National Institute of Technology Patna convey warm greetings for your time and effort to submit paper in the Fifth edition of the International Conference on Emerging Frontiers in Electrical and Electronic Technologies (ICEFEET-2026) is being organised at the Department of Electrical Engineering, NIT Patna on 09-10, July 2026.

We are glad to convey that your paper is accepted. The information regarding your submission may be found as follows:

Paper ID: 745

Paper Title: Performance Analysis of Boost Converter using Soft Switching Schemes

Decision: Accept

NOTE: You must check reviewers' comments by logging into CMT account and prepare the revised paper strictly conforming to the conference template given in our website. It is mandatory to address the reviewers' and meta-reviewer's feedback and incorporate the same in the Final version of your paper.

The subsequent steps like the camera-ready paper submission and conference registration process will be updated on the website from time to time.

--

Thanks and regards,

ICEFEET 2026 Organizing Team

National Institute of Technology Patna (NIT Patna)

email: [icefeet@nitp.ac.in](mailto:icefeet@nitp.ac.in)

website: <http://citac.mnnitp.ac.in/icefeet-2026/home>